Inorganic Chemistry

Article

pubs.acs.org/IC

Novel Dinuclear Platinum(II) Complexes Containing Mixed Nitrogen–Sulfur Donor Ligands

Stephanie Hochreuther,[†] Ralph Puchta,[†,‡] and Rudi van Eldik*,[†]

[†]Inorganic Chemistry, Department of Chemistry and Pharmacy, University of Erlangen-Nürnberg, Egerlandstrasse 1, 91058 Erlangen, Germany

[‡]Computer Chemistry Center, Department of Chemistry and Pharmacy, University of Erlangen-Nürnberg, Nägelsbachstrasse 25, 91052 Erlangen, Germany

Supporting Information

ABSTRACT: A series of novel dinuclear platinum(II) complexes were synthesized containing a mixed nitrogen–sulfur donor bidentate chelate system in which the two platinum centers are connected by an aliphatic chain of variable length. The bidentate chelating ligands were selected to stabilize the complex toward decomposition. The pK_a values and reactivity of the four synthesized complexes, namely, $[Pt_2(S^1,S^4\text{-bis(2-pyridylmethyl)-1,4-butanedithioether})(OH_2)_4]^{4+}$ (**4NSpy**), $[Pt_2(S^1,S^6\text{-bis(2-pyridylmethyl)-1,6-hexanedithioether})(OH_2)_4]^{4+}$ (**6NSpy**), $[Pt_2(S^1,S^8\text{-bis(2-pyridylmethyl)-1,8-octanedithioether})(OH_2)_4]^{4+}$ (**8NSpy**), and $[Pt_2(S^1,S^{10}\text{-bis(2-pyridylmethyl)-1,10-decanedithioether})(OH_2)_4]^{4+}$ (**10NSpy**), were investigated. This system is of special interest because only little is known about the substitution behavior of dinuclear platinum complexes that contain a bidentate chelate that forms part of the aliphatic bridging ligand. Moreover, the ligands as well as the dinuclear complexes were examined in terms of their cytotoxic activity, and the **10NSpy** complex was found to be active. Spectrophotometric acid–base titrations were performed to determine the pK_a values of all the coordinated water molecules. The substitution of coordinated water by thiourea was studied under pseudo-first-order conditions as a function of nucleophile concentration, temperature, and pressure, using stopped-flow techniques and UV–vis spectroscopy. The results for the dinuclear complexes were compared to those for the corresponding mononuclear reference complex $[Pt(methylthiomethylpyridine)(OH_2)_2]^{2+}$ (**Pt(mtp)**), by which the effect of the increasing aliphatic chain length of the bridged complexes could be investigated. The results indicate that there is a clear interaction between the two platinum centers, which becomes weaker as the chain length between the metal centers increases. Furthermore, differences and similarities of the N,S-system were compared to the corresponding dinuclear N,N-system studied previously in our group. In addition, quantum chemical calculations were performed to support the interpretation and discussion of the experimental data.

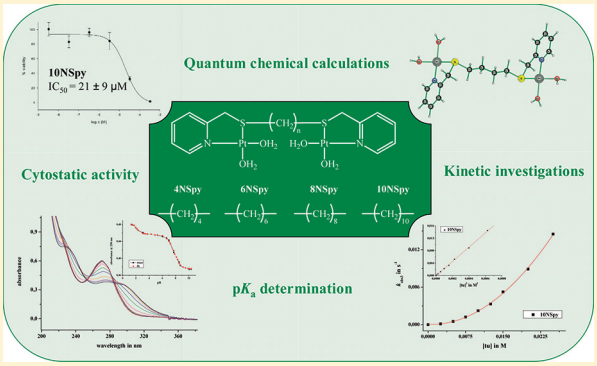

INTRODUCTION

During the past decades, numerous Pt-containing compounds have been synthesized, and their cytostatic activity has been analyzed.[1] The main goal was to create new possibilities for anticancer therapy. Since the discovery of the cytostatic activity of cisplatin, the first platinum containing anticancer drug, in 1969,[2,3] much more has been learned in terms of cytostatic properties of platinum drugs. Mononuclear Pt(II) as well as Pt(VI) compounds have been developed and improved step by step (Figure 1). Cisplatin was part of the first generation of Pt-containing drugs. Efforts to develop cisplatin analogues with reduced toxicity and a broader range of therapeutic activity led to the discovery of carboplatin (a second generation drug). By replacing chloride with 1,1-cyclobutanedicarboxylate, as new leaving group, carboplatin aquates slower compared to cisplatin and therefore is significantly less toxic,[4,5] but displays similar activity when used to treat ovarian cancer.[6−10] Another problem was the cross resistance of carboplatin to cisplatin, and as a consequence in a next step the spectator ligands were changed, which resulted in the development of numerous different compounds, for example, oxaliplatin (a third generation drug).[11,12] In oxaliplatin the two ammine ligands were replaced by a single bidentate ligand, namely, (1*R*,2*R*)-cyclohexane-1,2-diamine.[13] Oxaliplatin shows no cross-resistance to cisplatin and carboplatin because of a differently formed DNA adduct.[14] By synthesizing different platinum compounds, investigating their cytostatic activity and comparing the results, the so-called structure–activity relationship was summarized.[15] This postulation was helpful for further synthetic work to be able to predict cytostatic activity. Naturally, research always continues and scientists like Farrell and co-workers developed the so-called nonclassical platinum drugs,[16] which are multinuclear and therefore offer a completely different mechanism of binding to

Received: August 29, 2011
Published: November 15, 2011

   dx.doi.org/10.1021/ic2018902 | *Inorg. Chem.* 2011, 50, 12747–12761

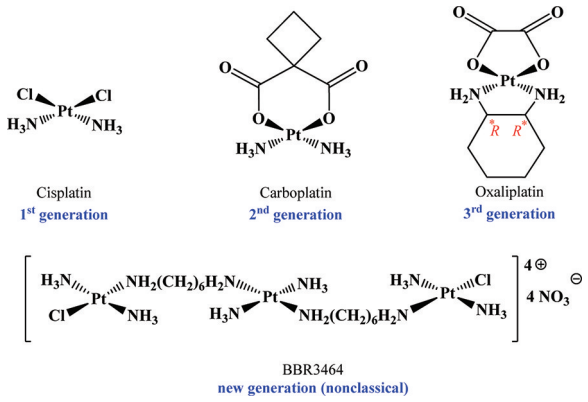

Figure 1. Selection of Pt(II)-based anticancer drugs, which have gained marketing approval for human use (upper row) or which have entered phase II clinical trials (BBR3464).

DNA, although some violate the classical structure−activity relationship.[17−21] BBR3464 is a trinuclear Pt(II) drug chosen as the lead agent from a family of di- and trinuclear complexes. It displays higher and faster uptake into cisplatin sensitive and resistant cells[22] and faster DNA binding.[23] However, the crucial point is the formation of a range of unique DNA adducts that are thought to be the mechanism by which it derives its potent cytotoxicity.

In the past almost all medicinal used platinum drugs contained exclusively nitrogenous donor ligands. Not until the past 10 years have S-containing donor ligands and their corresponding platinum complexes been synthesized. The group of Sadler for instance developed a sulfur analogue of the well-studied $Pt(H_2NCH_2CH_2NH_2)Cl_2$ complex, namely, $Pt(CH_3SCH_2CH_2SCH_3)Cl_2$, and Bugarčić et al. found the complex to be cytostatic active against MCF7 (breast cancer) cell lines.[24] Besides exclusively sulfur donor containing compounds, complexes with mixed spectator ligands have been developed.[25−27] For example the complex dichloro(2-methylthiomethylpyridine)platinum(II), **Pt(mtp)Cl$_2$**, is a complex with nitrogen as well as sulfur donor ligands. In the literature different synthetic pathways are described,[28−30] and the bidentate mixed N,S-complex was found to be a promising cytostatic agent.[31] Furthermore, the corresponding diaqua complex was recently studied in detail in our group.[32] Hardly any literature is presently available on di- or polynuclear Pt(II) complexes with S-containing donor ligands.

The present study is a continuation of earlier work performed in our group, where dinuclear nitrogen donor containing Pt(II) complexes were investigated.[33] We now switched from exclusively N-containing to mixed N- and S-containing dinuclear Pt(II) complexes. Figure 2 shows the novel complexes used in this study as well as their mononuclear analogue, which was also investigated in our group.[32] The complexes consist of a pyridyl unit (N-donor) and a thiomethylether unit (S-donor). The two Pt(II) centers are connected by an aliphatic chain of variable length. The dinuclear complexes are abbreviated according to their aliphatic chain length, the employed N,S-donor atoms, and the presence of a pyridine ring, namely, **4NSpy**, **6NSpy**, **8NSpy**, **10NSpy**, and **Pt(mtp)** for the mononuclear reference complex, respectively.

Usually, complexes with bidentate coordination spheres show higher cytostatic activity than their analogue with only one vacant coordination site.[34] In addition, it is known from multinuclear complexes that the DNA adducts of such complexes are

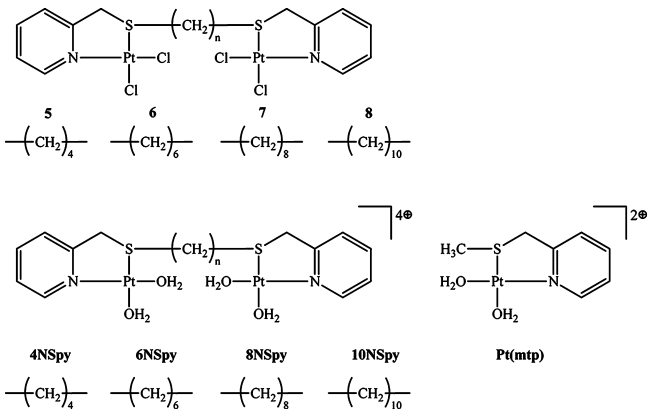

Figure 2. Structures of the studied dinuclear N,S−Pt(II) complexes (**NSpy system**) and their mononuclear analogue **Pt(mtp)**.

more flexible and long ranged, with a high degree of interstrand cross-links.[35] Furthermore, it is interesting to study the combination of a strong σ-donor and a π-acceptor within the same complex. Surprising results may show up as observed in the work of Hofmann et al.,[36] who combined pyridyl (π-acceptor) with benzyl moieties (σ-donor) within the same complex.

In the present work, we focused on the nature of the substitution reactions with thiourea and their dependence on the chain length of the complexes. We used thiourea as a strong S-containing nucleophile because of its good water solubility, high nucleophilicity, and neutral character. The high affinity of Pt(II) for sulfur is also of interest in terms of chemo-protective ability. Thiourea or methionine were especially used against nephrotoxicity, to suppress the coordination of platinum to S-containing proteins, which is responsible for several side effects.[37] We report thermodynamic (pK_a values) and kinetic data (rate and activation parameters) for the complexes studied, and used quantum chemical calculations to support the interpretation of the experimental results. The corresponding **Pt(mtp)** reference complex[32] and the previously obtained information on its kinetic behavior is useful for comparison with the here studied dinuclear system. In addition, cytostatic cell tests of all ligands and dinuclear complexes were carried out using the HeLa S3 cell line.

EXPERIMENTAL SECTION

Chemicals. The starting materials 2-picolyl chloride hydrochloride, the different alkyl dithiols, 1,10-decanedibromide, the nucleophile thiourea, trifluoromethanesulfonic (triflic) acid, and silver triflate were purchased from Acros Organics. Potassium tetrachloroplatinate(II) was obtained from Strem Chemicals. The deuterated chemicals, such as D_2O, deuterated triflic acid (CF_3SO_3D) and NaOD, were obtained from Deutero GmbH. All other used chemicals were of the highest purity commercially available and were used without further purification. For all preparations of aqueous solutions, ultra pure water was used.

Preparation of the (N,S)-Ligand System. S^1,S^4-bis(2-pyridylmethyl)-1,4-butanedithioether (**1**), S^1,S^6-bis(2-pyridylmethyl)-1,6-hexanedithioether (**2**), S^1,S^8-bis(2-pyridylmethyl)-1,8-octanedithioether (**3**), and S^1,S^{10}-bis(2-pyridylmethyl)-1,10-decanedithioether (**4**), were prepared according to a well-known procedure:[38] A sodium ethoxide solution was prepared by addition of 0.92 g (40 mmol) of sodium metal to 20 mL of dry ethanol at 0 °C followed by addition of the corresponding dithiol (5 mmol) and an ethanolic solution of 3.28 g (20 mmol) of 2-picolyl chloride hydrochloride, while keeping the temperature at 0−5 °C. The resulting suspension was allowed to reach room temperature, stirred for 30 min, followed by stirring for 2 h

dx.doi.org/10.1021/ic2018902 | Inorg. Chem. 2011, 50, 12747−12761

under reflux. The mixture was cooled to room temperature, and 50 mL of water was added to destroy remaining sodium ethoxide, and finally the ethanol was removed under reduced pressure. The product was extracted with dichloromethane (4 × 20 mL), the combined organic layers were dried over Na_2SO_4, and the product was obtained by removing the solvent under reduced pressure. The 4-(N,S)- and 6-(N,S)-ligands were obtained as orange oils, while the ligands with longer chains such as the 8-(N,S)- and 10-(N,S)-ligands were found to be lightly yellow solids. All ligands were characterized and identified by NMR spectroscopy and used for complex-formation without further purification.

The bridging reagent 1,10-decanedithiol (**4a**) is commercially not available and was therefore prepared following the reported procedure with slight modifications:[39] To a solution of 6.0 g (20 mmol) of 1,10-decanedibromide in 50 mL of ethanol, 3.2 g (42 mmol) of solid thiourea were added within 10 min and stirred under reflux overnight. The reaction mixture was then cooled to room temperature, treated dropwise with 90 mL of 10% NaOH solution and again refluxed (110 °C) for 3 h. After cooling to room temperature, the mixture was diluted with 100 mL of a 1 M HCl solution until pH 7 was reached. The product was extracted with diethyl ether (2 × 200 mL) and obtained as colorless oil after evaporation of the solvent. The crude product was identified by NMR spectroscopy and used for the next step without further purification.

1: $C_{16}H_{20}N_2S_2$ (M = 304.5 g/mol). ^{1}H NMR ($CDCl_3$, 298.2 K): δ 8.43 (d, $^3J_{HH}$ = 4.8 Hz, 2H), δ 7.56 (dt, $^3J_{HH}$ = 7.7 Hz, $^4J_{HH}$ = 1.7 Hz, 2H), δ 7.27 (d, $^3J_{HH}$ = 7.7 Hz, 2H), δ 7.06 (dd, $^3J_{HH}$ = 4.8 Hz, $^4J_{HH}$ = 7.7 Hz, 2H), δ 3.73 (s, 4H), δ 2.38 (t, $^3J_{HH}$ = 6.5 Hz, 4H), δ 1.59−1.52 (m, 4H). ^{13}C NMR ($CDCl_3$, 298.2 K): δ 158.7, 149.0, 136.5, 122.8, 121.6, 37.9, 30.9, 28.0.

2: $C_{18}H_{24}N_2S_2$ (M = 332.5 g/mol). ^{1}H NMR ($CDCl_3$, 298.2 K): δ 8.43 (d, $^3J_{HH}$ = 4.8 Hz, 2H), δ 7.62 (dt, $^3J_{HH}$ = 8.5 Hz, $^4J_{HH}$ = 1.7 Hz, 2H), δ 7.34 (d, $^3J_{HH}$ = 7.8 Hz, 2H), δ 7.12 (dd, $^3J_{HH}$ = 4.8 Hz, $^4J_{HH}$ = 7.8 Hz, 2H), δ 3.79 (s, 4H), δ 2.44 (t, $^3J_{HH}$ = 7.4 Hz, 4H), δ 1.55−1.46 (m, 4H), δ 1.35−1.26 (m, 4H). ^{13}C NMR ($CDCl_3$, 298.2 K): δ 158.9, 149.0, 136.5, 122.9, 121.7, 38.1, 31.5, 28.9, 28.2.

3: $C_{20}H_{28}N_2S_2$ (M = 360.6 g/mol). ^{1}H NMR ($CDCl_3$, 298.2 K): δ 8.43 (d, $^3J_{HH}$ = 4.8 Hz, 2H), δ 7.56 (dt, $^3J_{HH}$ = 8.5 Hz, $^4J_{HH}$ = 1.6 Hz, 2H), δ 7.29 (d, $^3J_{HH}$ = 7.8 Hz, 2H), δ 7.06 (dd, $^3J_{HH}$ = 4.8 Hz, $^4J_{HH}$ = 7.8 Hz, 2H), δ 3.75 (s, 4H), δ 2.39 (t, $^3J_{HH}$ = 7.3 Hz, 4H), δ 1.50−1.41 (m, 4H), δ 1.28−1.14 (m, 8H). ^{13}C NMR ($CDCl_3$, 298.2 K): δ 158.9, 149.0, 136.4, 122.8, 121.6, 38.1, 31.5, 29.0, 28.8, 28.5.

4a: $C_{10}H_{24}S_2$ (M = 206.4 g/mol). ^{1}H NMR ($CDCl_3$, 298.2 K): δ 2.46 (t, $^2J_{HH}$ = 7.2 Hz, 4H), δ 1.60−1.50 (m, 4H), δ 1.35−1.20 (m, 12H). ^{13}C NMR ($CDCl_3$, 298.2 K): δ 34.01, 29.41, 29.02, 28.34, 24.63.

4: $C_{22}H_{32}N_2S_2$ (M = 388.6 g/mol). ^{1}H NMR ($CDCl_3$, 298.2 K): δ 8.44 (d, $^3J_{HH}$ = 4.8 Hz, 2H), δ 7.57 (dt, $^3J_{HH}$ = 8.5 Hz, $^4J_{HH}$ = 1.7 Hz, 2H), δ 7.30 (d, $^3J_{HH}$ = 7.8 Hz, 2H), δ 7.07 (dd, $^3J_{HH}$ = 4.8 Hz, $^4J_{HH}$ = 7.8 Hz, 2H), δ 3.75 (s, 4H), δ 2.40 (t, $^3J_{HH}$ = 7.3 Hz, 4H), δ 1.52−1.42 (m, 8H), δ 1.19−1.12 (m, 8H). ^{13}C NMR ($CDCl_3$, 298.2 K): δ 159.0, 149.1, 136.5, 122.9, 121.7, 38.1, 31.6, 29.3, 29.1, 29.0, 28.7.

Synthesis of the (N,S)-Complex System. [Pt_2(S^1,S^4-bis(2-pyridylmethyl)-1,4-butanedithioether)Cl_4] (**5**), [Pt_2(S^1,S^6-bis(2-pyridylmethyl)-1,6-hexanedithioether)Cl_4] (**6**), [Pt_2(S^1,S^8-bis(2-pyridylmethyl)-1,8-octanedithioether)Cl_4] (**7**), and [Pt_2(S^1,S^{10}-bis(2-pyridylmethyl)-1,10-decanedithioether)Cl_4] (**8**) were synthesized according to a literature method.[40] To 0.48 mmol of the corresponding ligands (**1**−**4**), a solution of 400 mg (0.96 mmol) of K_2PtCl_4 in water was slowly added using a dropping funnel, under vigorous stirring at room temperature. The reaction mixture was further stirred until the characteristic red color of dissolved K_2PtCl_4 disappeared (3−6 h). The resulting yellow precipitate was filtered off, washed with water, ethanol, and diethyl ether, and dried under vacuum. During complexation the SR_2−sulfur donor atom becomes a stereogenic center and three configurations, namely, *R,R*; *S,S* and *R,S* are possible. We were not able to isolate single diastereomers because of rapid (S)-inversion at the sulfur atom (for further discussion, see kinetic measurements), and consequently used a mixture of the generated species in all measurements.

5: Yield: 337 mg (0.40 mmol, M = 836.4 g/mol, 84%). Anal. Calcd for $C_{16}H_{20}Cl_4N_2Pt_2S_2$: C, 22.97; H, 2.41; N, 3.35; S, 7.67%. Found: C, 22.90; H, 2.40; N, 3.25; S, 7.92%. ^{1}H NMR (dmso-d_6, 298.2 K): δ 9.38 (d, $^3J_{HH}$ = 4.9 Hz, 2H), δ 8.16 (t, $^3J_{HH}$ = 7.7 Hz, 2H), δ 7.80 (d, $^3J_{HH}$ = 7.7 Hz, 2H), δ 7.54 (m, 2H), δ 4.76 (d, AB-spin system, $^2J_{HH}$ = 17.0 Hz, 2H), δ 4.48 (d, AB-spin system, $^2J_{HH}$ = 17.0 Hz, 2H), δ 2.88−2.67 (m, 4H), δ 1.91−1.76 (m, 4H). MS-FAB (NBA, 70 eV) 801 $[M-Cl]^+$.

6: Yield: 278 mg (0.32 mmol, M = 864.5 g/mol, 67%). Anal. Calcd for $C_{18}H_{24}Cl_4N_2Pt_2S_2$: C, 25.01; H, 2.80; N, 3.24; S, 7.42%. Found: C, 24.83; H, 2.77; N, 2.96; S, 7.61%. ^{1}H NMR (dmso-d_6, 298.2 K): δ 9.41 (d, $^3J_{HH}$ = 5.5 Hz, 2H), δ 8.17 (t, $^3J_{HH}$ = 7.7 Hz, 2H), δ 7.82 (d, $^3J_{HH}$ = 7.7 Hz, 2H), δ 7.56 (m, 2H), δ 4.76 (d, AB-spin system, $^2J_{HH}$ = 17.0 Hz, 2H), δ 4.48 (d, AB-spin system, $^2J_{HH}$ = 17.0 Hz, 2H), δ 2.89−2.65 (m, 4H), δ 1.71−1.56 (m, 4H), δ 1.44−1.34 (m, 4H). MS-FAB (NBA, 70 eV) 830 $[M-Cl]^+$.

7: Yield: 300 mg (0.34 mmol, M = 892.6 g/mol, 70%). Anal. Calcd for $C_{20}H_{28}Cl_4N_2Pt_2S_2$: C, 26.91; H, 3.16; N, 3.14; S, 7.14%. Found: C, 27.02; H, 3.19; N, 2.88; S, 7.43%. ^{1}H NMR (dmso-d_6, 298.2 K): δ 9.40 (d, $^3J_{HH}$ = 5.4 Hz, 2H), δ 8.16 (t, $^3J_{HH}$ = 7.8 Hz, 2H), δ 7.81 (d, $^3J_{HH}$ = 7.8 Hz, 2H), δ 7.55 (m, 2H), δ 4.75 (d, AB-spin system, $^2J_{HH}$ = 17.0 Hz, 2H), δ 4.48 (d, AB-spin system, $^2J_{HH}$ = 17.0 Hz, 2H), δ 2.86−2.64 (m, 4H), δ 1.75−1.59 (m, 4H), δ 1.40−1.31 (m, 4H), δ 1.22−1.15 (m, 4H). MS-FAB (NBA, 70 eV) 857 $[M-Cl]^+$.

8: Yield: 358 mg (0.39 mmol, M = 920.6 g/mol, 81%). Anal. Calcd for $C_{22}H_{32}Cl_4N_2Pt_2S_2$: C, 28.70; H, 3.50; N, 3.04; S, 6.97%. Found: C, 28.44; H, 3.39; N, 2.82; S, 6.97%. ^{1}H NMR (dmso-d_6, 298.2 K): δ 9.40 (d, $^3J_{HH}$ = 5.4 Hz, 2H), δ 8.16 (t, $^3J_{HH}$ = 7.8 Hz, 2H), δ 7.81 (d, $^3J_{HH}$ = 7.8 Hz, 2H), δ 7.55 (m, 2H), δ 4.76 (d, AB-spin system, $^2J_{HH}$ = 17.0 Hz, 2H), δ 4.49 (d, AB-spin system, $^2J_{HH}$ = 17.0 Hz, 2H), δ 2.86−2.64 (m, 4H), δ 1.75−1.59 (m, 4H), δ 1.40−1.31 (m, 4H), δ 1.22−1.15 (m, 4H). MS-FAB (NBA, 70 eV) 885 $[M-Cl]^+$.

Preparation of the Complex Solutions.[41] Solutions of the aqua complexes were prepared by suspending a defined amount of the corresponding chloro complexes **5**−**8** in 0.001 M triflic acid and adding a stoichiometric excess of silver triflate (4.1 equiv) with respect to the chloro ligands. The mixture was then stirred in the dark for at least 2 days at 45 °C, which led to the formation of silver chloride. The precipitated silver chloride was filtered off, and the pH of the resulting solution was increased to 11 by addition of small amounts of 0.1 M NaOH. This led to the formation of brown silver oxide (from the excess silver triflate), which was then removed with a Millipore filter, and the pH of the remaining solution was adjusted to pH 2 with triflic acid to give the desired complex concentration of 0.2 mM. For all kinetic investigations the pH of the solution was kept at 2, and the ionic strength was adjusted to I = 0.01 M (triflic acid). After aquation, the complex solutions were characterized using NMR spectroscopy and mass spectrometry (see further Discussion).

Cytostatic Tests. Cell tests for all four dinuclear Pt(II) tetrachloro complexes (**5**−**8**) and for all ligands (**1**−**4**) were performed. The cytotoxicity of the complexes was studied using the AlamarBlue assay in the human cervix carcinoma cell line HeLa S3. The AlamarBlue assay is characterized by its linearity and its high sensitivity, while its handling is less error prone in contrast to the MTT assay. Living cells reduce the sodium salt of the dark blue, nonfluorescent dye resazurin (7-hydroxy-3*H*-phenoxazin-3-one-10-oxide) to the pink, highly fluorescent resurufin (7-hydroxy-3*H*-phenoxazin-3-one). In the commonly used MTT assay, the formed formazan is insoluble in the cell-culture medium and requires dimethyl sulfoxide (dmso, DMSO) as an additional solubilizer. The handling of the AlamarBlue assay is thus much simpler, readout by fluorescent detection is directly achieved without additional steps.[42] Cells were cultivated at 37 °C and 5% CO_2 atmosphere in DMEM medium (Gibco) with 10% FCS (Biochrome AG) and 1% Pen/Strep (GIBCO) added. Cells were split twice per week. For the assay, cells were seeded in 96-well plates (4 000 cells/well) and allowed to attach for 24 h. Complexes to be tested were dissolved in a suitable amount of DMSO. Different concentrations were prepared by serial dilution with medium to give final concentrations with a maximum DMSO content of 1%. The cells were then incubated for 48 h with 100 μL each of above dilution series. After removal of the medium, AlamarBlue solution (10 μL (BioSource Europe) diluted with

dx.doi.org/10.1021/ic2018902 | Inorg. Chem. 2011, 50, 12747−12761

90 μL DMEM medium) was directly added, and the cells were incubated for 90 min. After excitation at 530 nm, fluorescence at 590 nm was measured using a Synergy HT Microplate Reader (Bio-TEK). Cell viability is expressed in percent with respect to a control containing only pure medium and 1% DMSO incubated under identical conditions. All experiments were repeated two times with each experiment done in four replicates. The resulting curves were fitted using Sigma plot 10.0 (Systat Software, Inc. 2006).

Instrumentation and Measurements. NMR spectroscopy (Bruker Avance DPX 300) and a Carlo Erba Elemental Analyzer 1106 were used for ligand and chloro complex characterization and chemical analysis, respectively. ^{195}Pt-NMR measurements were performed on a Bruker Avance DRX 400WB with K_2PtCl_4 (in D_2O/CF_3SO_3D) as reference (δ = −1620 ppm). Mass spectrometric measurements were performed on an UHR-TOF Bruker Daltonik (Bremen, Germany) maXis, an ESI-TOF mass spectrometer capable of a resolution of at least 40000 fwhm used by the group of Prof. Ivana Ivanović-Burmazović at the University of Erlangen-Nürnberg. A Varian Cary 1G spectrophotometer equipped with a thermostatted cell holder was used to record UV−vis spectra for the determination of the pK_a values of the aqua complexes. Kinetic measurements on fast reactions were carried out on an Applied Photophysics SX 18MV stopped-flow instrument and for the study of slow reactions a Shimadzu UV-2010PC spectrophotometer with a thermo-electrically controlled cell holder was used. Experiments at elevated pressure were performed on a laboratory-made high-pressure stopped-flow instrument for fast reactions.[43] The temperature of the instruments was controlled throughout all kinetic experiments to an accuracy of ±0.1 °C. The values of the reported pseudo-first-order rate constants are the average of at least four kinetic measurements.

Computational Details. We performed B3LYP/LANL2DZp hybrid density functional calculations, that is, with pseudopotentials on the heavy elements and the valence basis set augmented with polarization functions.[44−50] During the optimization of the structures no constraints other than symmetry were applied. In addition, the resulting structures were characterized as minima by computation of vibrational frequencies. The Gaussian 03 suite of programs was used throughout.[51]

RESULTS AND DISCUSSION

Characterization of the Tetraaqua Complexes. The chloro complexes of the **NSpy** system were fully characterized as reported in the Experimental Section. However, a closer look at the resulting solution has to be taken following aquation and removal of chloride ions. Aquation of the chloro complexes involves an increase in pH up to 11. This high pH leads to deprotonation of the water ligands and probably to the formation of μ-OH dimers. After slow addition of concentrated triflic acid, the pH is decreased to 2 and the dimers are expected to decompose. To clarify the composition of the solution after removing the chloride ions, we performed NMR spectroscopic and mass spectrometric measurements.

For NMR measurements the aquation was carried out as mentioned in the Experimental Section using D_2O, deuterated triflic acid (CF_3SO_3D), and NaOD instead of H_2O, triflic acid, and NaOH. After aquation the pH* (without correction) of the samples was adjusted using drops of concentrated deuterated triflic acid to obtain a pH* of 2. We performed ^{1}H- and ^{195}Pt-NMR measurements to detect the species present in solution and to check the purity of the solution. By way of example, Figures 3 and 4 show the ^{1}H- and ^{195}Pt-NMR spectra of **6NSpy**. The spectra of the three remaining **NSpy** complexes are shown in Figures S1−S6 of the Supporting Information. The ^{1}H NMR spectrum clearly shows evidence for complex-formation because of the presence of two doublets at 4.45 and 4.19 ppm, which represent the AB-spin system of the CH_2

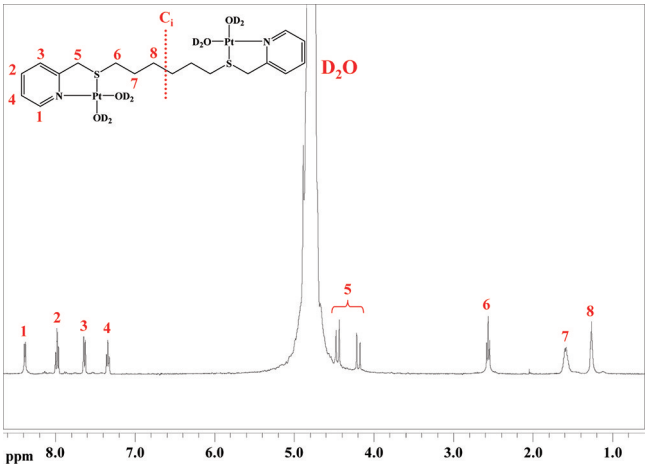

Figure 3. ^{1}H NMR spectrum of the **6NSpy** complex at pH 2 (D_2O/CF_3SO_3D).

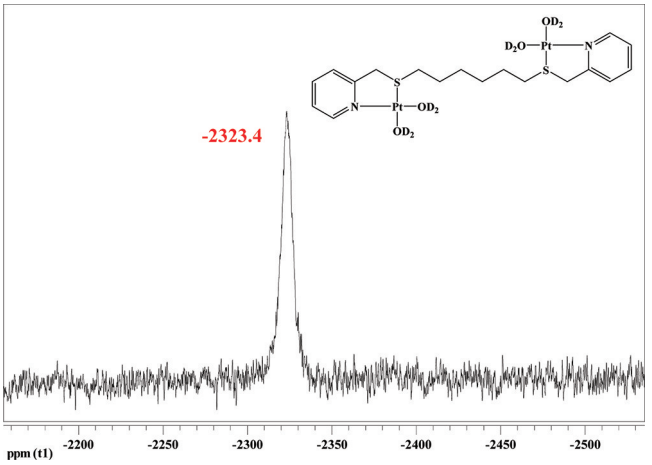

Figure 4. ^{195}Pt-NMR spectrum of the **6NSpy** complex at pH 2 (D_2O/CF_3SO_3D).

group "5" between the pyridine ring and bridge (see drawing in Figure 3), and demonstrates the purity of the aqua complex solution. The concentration of the solution is quite low, which can be seen in the large D_2O solvent peak at 4.79 ppm.

Dimeric as well as OH-containing species can be analyzed using ^{195}Pt-NMR. In general, bridged μ-OH dimers show a clear shift to lower fields because of deshielding of the Pt(II) center.[52] Furthermore, different species present would lead to more than one signal in the spectra. The **Pt(mpt)** chloro complex, [Pt(2-methylthiomethylpyridine)Cl_2], as mononuclear analogue was used as reference to locate the ppm region for the subsequent measurements of the dinuclear system. **Pt(mpt)** was measured in dmso-d_6 because of the poor solubility of the neutral chloro complex in D_2O and exhibits one peak at −2780.5 ppm and its reference-spectrum is reported in Figure S7 of the Supporting Information. The ^{195}Pt-NMR measurements were performed in two ppm ranges from −2000 to −3000 ppm, where the signals of the dinuclear system are supposed to occur, and also at lower field from −1000 to −2000 ppm to check for the presence of dimeric species. Because of the symmetry of the dinuclear system, the two Pt(II) centers are equivalent and exhibit the same chemical shift. According to this, exactly one peak was observed in the ^{195}Pt-NMR spectra, which can be seen in Figure 4 for the

dx.doi.org/10.1021/ic2018902 | Inorg. Chem. 2011, 50, 12747−12761

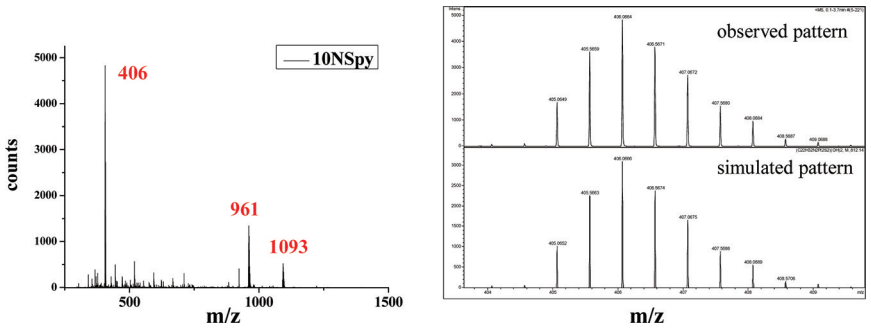

Figure 5. Mass spectrum of the **10NSpy** complex at pH 2 (left) and the isotopic pattern as well as the simulated pattern for the main peak at m/z = 406 (right).

6NSpy complex. We note that because of the low solubility of the **10NSpy** complex, the poor signal-to-noise ratio of the ^{195}Pt spectrum hampers the analysis. However, only one signal is recognizable and furthermore the ^{1}H spectrum also clearly shows the presence of only one species. No signals were observed in the low field range. The chemical shifts of the dinuclear Pt(II) complexes are independent of the chain length and appear in the same region. We found values of −2324.0 ppm (**4NSpy**), −2323.4 ppm (**6NSpy**), −2324.3 ppm (**8NSpy**), and −2323.0 ppm (**10NSpy**), which are in good agreement for platinum complexes in the oxidation state 2+ and bidentate coordination spheres.[52]

In addition, mass spectrometric measurements were performed and in general confirm the information obtained from the NMR measurements. As an example, Figure 5 depicts the mass spectrum in the m/z range of 200−1500 for the **10NSpy** complex. The main peaks can be found at m/z = 406 (2+), 961 (1+), and 1039 (1+), which consist of $[(C_{22}H_{32}N_2Pt_2S_2)(OH)_2]$, $[(C_{22}H_{32}N_2Pt_2S_2)(OH)_2(CF_3SO_3)]$, and $[(C_{22}H_{32}N_2Pt_2S_2)(OH)(CF_3SO_3)_2]$ and represent fragments of the **10NSpy** aqua complex. Furthermore, Figure 5 depicts the isotopic pattern at m/z = 406 and its corresponding simulated pattern (also Figures S8−S13, Supporting Information).

The mass spectra of all aqua complexes show similar fragments for the entire dinuclear system, that is, no dimers or polymers were observed. Such species would exhibit a different isotopic pattern and would have been detected during simulation of each peak. Intramolecular μ-OH species can not be distinguished from normal OH-coordinated species in the mass spectrometric measurements, since they exhibit the same isotopic pattern, but can be excluded on the basis of the NMR spectra. The appearance of hydroxo ligands on the complex observed in the mass spectra is due to the ionization of coordinated water. Beside the complex peaks, a few single peaks can be found that belong to organic fragments generated during the evaporation procedure (180 °C).

On the basis of the NMR and mass spectrometric measurements, we conclude that after aquation and increasing the pH to 11, the possible generated hydroxo and μ-OH bridged species decompose during acidification of the solution. Consequently, the tetraaqua complexes are predominantly present in solution at pH 2, which could also be verified by performing a pH speciation for the complete dinuclear **NSpy** system (see further discussion).

We also tried to isolate crystals for the aqua and chloro complexes, but unfortunately were not successful. The chloro complexes are neutral compounds and poorly soluble in any common solvent. Furthermore, the aqua complexes were treated with different kinds of counteranions, such as ClO_4^-, BF_4^-, PF_6^-, and NTf_2^{2-}, but no crystals were obtained.

pK_a Determination of the Tetraaqua Complexes. For further mechanistic clarification, it is important to obtain information on the acidity of the coordinated water ligands and therefore on the reactivity of the aqua complexes. For this reason spectrophotometric pH titrations with NaOH as base in the pH range of 1−10 were performed. The spectrophotometric pK_a determination was done using a Hellma optical cell for flow-through measurements attached to a peristaltic pump. Thereby, it was necessary to keep the concentration of the complex solution constant, to avoid absorbance corrections because of dilution. This can be achieved by using a large volume of 100 mL complex solution during the titration. Starting at pH 1, the pH was increased by addition of small portions of solid NaOH to the solution until a pH of 3 was reached. For further increase in pH, a series of NaOH solutions of different concentrations were used. The consecutive pH changes were obtained by dipping a needle into these NaOH solutions and then in the complex solution. After each addition of base, samples of 500 μL were taken from the complex solution, and the pH was measured at 25 °C using an InLab Semi-Micro pH electrode. This electrode was calibrated using standard buffer solutions at pH 4, 7, and 10, purchased from Fisher Scientific. Afterward the samples were discarded because of a possible chloride ion contamination coming from the pH electrode. Each pK_a titration was performed at least two times and an average of both values was taken. The pH dependence of the aqua complex was monitored by UV−vis spectroscopy. The so-obtained data were analyzed using the Specfit Global Analysis software. Specfit is a multivariant data analysis program for modeling and fitting of chemical kinetics and a variety of equilibrium titrations that are obtained from multiwavelength spectrophotometric measurements. An important advantage of this program is the inclusion of all the data measured as a function of wavelength for the calculated pK_a values.

The pK_a values were determined by probing different models for the systems studied. The model selected was that which gave the best statistical fit. A very low complex concentration of 0.05 mM was used during the pH titration to prevent dimer or polymer formation, since it is known from the literature that μ-OH bridged dimers, trimers, or tetramers can accumulate in solution at higher pH.[53−55] Because of the dinuclear system, a local high concentration can lead to intramolecular ring-closure through μ-OH bridges during the pH titration. Trials were made to fit the spectrophotometric data assuming the formation of a ring-closed dimer at higher pH, but this resulted in a very poor fit of the data.

dx.doi.org/10.1021/ic2018902 | Inorg. Chem. 2011, 50, 12747−12761

Figure 6 (and Figures S14–S16, Supporting Information) shows a typical example for **8NSpy** of a titration with its

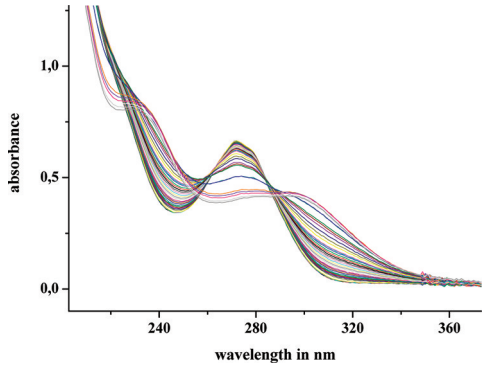

Figure 6. UV–vis spectra recorded for 0.05 mM **8NSpy** in the pH range 1–10 at 25 °C.

spectral changes recorded as a function of pH. The obtained pK_a values for the coordinated water ligands are summarized in Table 1. The fit-report for each complex is summarized in Tables S1–S4 of the Supporting Information.

In general, we found four pK_a values for the platinum bound water molecules for **4NSpy**, **6NSpy**, and **8NSpy**. The **10NSpy** complex with the longest methyl chain shows only two pK_a values. Plots of absorbance versus pH illustrate this fact. Figure 7 depicts the absorbance traces at one specific wavelength for all four complexes. Although this wavelength exhibits only small spectral changes, it was selected on purpose because in this region the absorbance spectra reflected best the change from one species into another. Figures S17–S20 (Supporting Information) report the data for three other wavelengths by way of further examples. We note that not every deprotonation step is visible at each wavelength.

A similar behavior is already known from the work of Farrell et al.[56] and was also observed in our group.[33,57] The determination of pK_a values for polynuclear Pt(II) complexes, where the relevant Pt centers are far away from each other, show only one pK_a value for two symmetrically equivalent water molecules. Thus, we assume for the complexes studied in this work, that on reaching a chain length of 10 methylene groups (distance between Pt–Pt = 18.40 Å (B3LYP/LANL2DZp)), it is not possible to differentiate between the two metal centers in terms of their acidity anymore. The dinuclear **10NSpy** complex behaves like two mononuclear complexes and shows only two pK_a values for a total of four water molecules. For better comparison with the other dinuclear complexes, we entitled the deprotonation of the first two water molecules trans to the pyridine nitrogen as pK_{a1} and the second deprotonation of the last two water molecules trans to the sulfur as pK_{a3} in Table 1. It is noticeable that the two pK_a values for **10NSpy** and **Pt(mtp)** differ in the first as well as in the second value (see Table 1). The **10NSpy** complex behaves like the mononuclear complex, but it is and remains dinuclear with an overall charge of 4+ and a

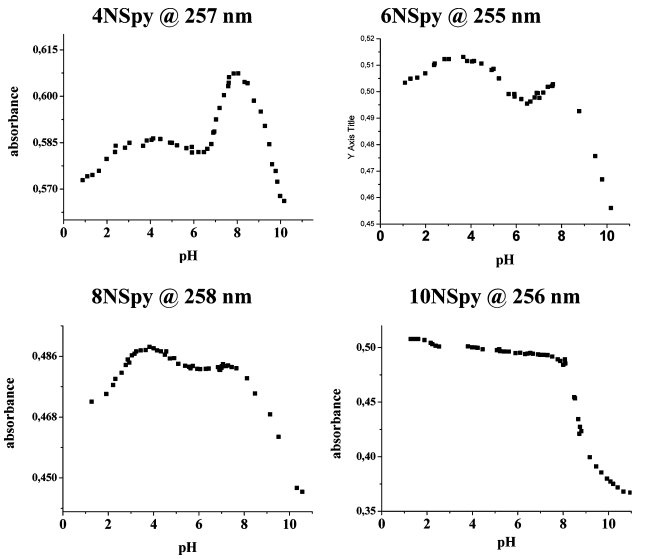

Figure 7. Plots of absorbance versus pH at specific wavelengths for the **NSpy** complex system.

methylene chain with an inductive effect. This of course has an influence on the pK_a values and leads to a decrease in pK_{a1} because of a higher positive charge of the tetra-aqua complex, and to an increase in pK_{a3} because of the electron donating effect of the aliphatic chain trans to the second deprotonated water molecule.

Since the complex system includes two different type of donors, namely, an aromatic pyridine unit with π-accepting ability and a sp^3-hybridized thioether unit (SR_2) with strong σ-donating ability, it is possible to distinguish which water molecule is deprotonated first. The sulfur donor with its strong σ-donor effect labilizes the water molecule in the trans position, such that the Pt–O bond trans to sulfur is elongated, which leads to a higher pK_a value. Moreover, it is known from previous work that through the presence of an in-plane pyridine unit in the chelate system, the electron density on the Pt(II) center and the hydroxo ligand is stabilized better by the electron withdrawing ability of the π-accepting pyridine ring.[58] Consequently, the water molecule trans to the pyridine nitrogen donor is deprotonated first and the resulting hydroxo ligand with its negative charge can perfectly be stabilized trans to the pyridine donor. Scheme 1 shows the proposed stepwise deprotonation steps for the pH dependence of the dinuclear system.

As mentioned before, the results shown in Table 1 indicate a correlation between the pK_a values and the chain length of the complexes. We found lower pK_{a1} values for the dinuclear N,S-system compared to the **Pt(mtp)** complex. This can be explained by the higher charge of 4+ compared to 2+ and was also found for the corresponding dinuclear N,N-system studied in our group before.[33] The pK_{a1} value is very similar for all dinuclear complexes with a slight increase on going from **4NSpy** to **10NSpy**. This effect was also observed for the

Table 1. Summary of pK_a Values Obtained for the Stepwise Deprotonation of Platinum Bound Water

	4NSpy	6NSpy	8NSpy	10NSpy		Pt(mtp)[32]
pK_{a1}	2.16 ± 0.01	2.38 ± 0.03	2.32 ± 0.01	2.46 ± 0.07	pK_{a1}	3.15 ± 0.03
pK_{a2}	5.22 ± 0.02	5.09 ± 0.06	4.86 ± 0.09			
pK_{a3}	7.14 ± 0.03	7.44 ± 0.06	7.86 ± 0.03	8.45 ± 0.07	pK_{a2}	6.84 ± 0.07
pK_{a4}	9.33 ± 0.03	9.21 ± 0.03	9.23 ± 0.03			

dx.doi.org/10.1021/ic2018902 | Inorg. Chem. 2011, 50, 12747–12761

Scheme 1. Proposed Stepwise Deprotonation for the pH Dependence of the Dinuclear System

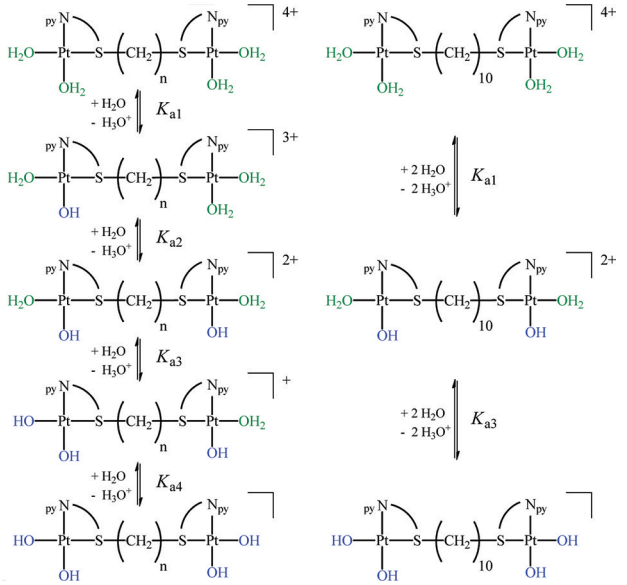

corresponding N,N-complex system,[33] and we suggest that the slight increase arises from a decrease in communication between the two Pt(II) centers accompanied by a decrease in the localized charge. We want to note that this small decrease in acidity is a result of charge effects and not of σ-donation by the aliphatic chains. The second deprotonation step occurs trans to the pyridine unit at the second Pt(II) center, and the pK_{a2} values are significantly higher compared to pK_{a1}. This effect can be ascribed to the change in overall charge from 4+ to 3+ and therefore to less electrophilic metal centers. As mentioned above, **10NSpy** shows no second deprotonation step in this pH area since it is not possible to distinguish between the two water molecules in each Pt(II) center. In addition, it is noticeable that the differences between pK_{a1} and pK_{a2} become smaller with increasing chain length (about 0.2 units for each additional two CH_2 groups). This again corroborates earlier work performed in our group.[33,57] As mentioned above, the effect of charge addition decreases as the distance between the Pt(II) centers becomes longer. This effect explains why with increasing chain length the difference between pK_{a1} and pK_{a2} becomes smaller.

At this stage both water ligands trans to pyridine are deprotonated, and the overall charge of the diaqua-dihydroxo species is 2+. The third deprotonation step now occurs trans to the sulfur donor. Because of the decreased overall charge, the pK_{a3} values are higher compared to those for the first two steps. As seen in Table 1, the pK_{a3} values are drastically influenced by the aliphatic chain length. The labilizing effect of the sulfur donor is accompanied by the inductive effect of the methyl chain. With increasing chain length the SR_2 unit receives more electron density and therefore exhibits a stronger σ-donor effect on the trans localized water molecule. Consequently, the water molecule becomes more labilized and the pK_{a3} values increase in the order **4NSpy** < **6NSpy** < **8NSpy** < **10NSpy**. Although the **10NSpy** complex offers only two pK_a values, it fits perfectly into the series and shows the highest pK_{a3} value.

Naturally, the final deprotonation step shows the highest pK_{a4} values. We found very similar values for the three complexes **4NSpy**, **6NSpy**, and **8NSpy**, and assume that the presence of three hydroxo ligands in the complex overrules the inductive effect of the aliphatic chain. Therefore, the pK_{a4} values are independent of the chain length. We want to note that the difference between pK_{a3} and pK_{a4} becomes smaller with increasing chain length as seen in Table 1. This again is a charge effect as mentioned above.

Finally, we want to discuss the relatively low pK_{a1} values for the dinuclear **NSpy** complexes as compared to the corresponding dinuclear **NNpy** system (for more information concerning the **NNpy** system see ref 33). Such low pK_a values for platinum bound water molecules are known in the literature. For example, Soldatović et al. determined a pK_{a1} value for a mononuclear N,S−Pt(II) complex of 3.49,[59] but offered no explanation for the relatively low value. To find similarities and differences in the **NSpy** and **NNpy** systems, we took a closer look at the geometry using quantum chemical calculations. We simulated the first two deprotonation steps to end at the 2+ charged diaqua-dihydroxo species for all dinuclear complexes. From a comparison of the tetraaqua species with the diaqua-dihydroxo species of the **4NSpy** with the **4NNpy** complexes as shown in Table 2, and also for the other complexes in Tables S5−S7 (Supporting Information), the lengths of the Pt−O bond trans to the pyridine nitrogen are essentially the

Table 2. Calculated Bond Lengths and Angles (B3LYP/LANL2DZp) for the 4NSpy and 4NNpy Complexes and for the Corresponding Deprotonated Species

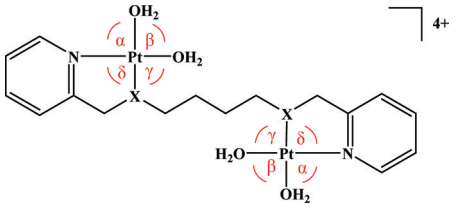

	4NSpy $[Pt_2(OH_2)_4]^{4+}$	**4NNpy** $[Pt_2(OH_2)_4]^{4+}$	**4NSpy** $[Pt_2(OH_2)_2(OH)_2]^{2+}$	**4NNpy** $[Pt_2(OH_2)_2(OH)_2]^{2+}$
α (deg)	92.3	94.4	100.2	102.5
β (deg)	85.4	97.7	76.3	77.7
γ (deg)	96.3	95.6	97.4	97.4
δ (deg)	85.8	82.2	86.1	82.3
d Pt−X (Å)	2.31	2.07	2.28	2.05
d Pt−N_{py} (Å)	2.01	2.00	2.07	2.06
d Pt−$O_{trans\ X}$ (Å)	2.16	2.13	2.15	2.12
d Pt−$O_{trans\ py}$ (Å)	2.13	2.15	1.99	2.00

dx.doi.org/10.1021/ic2018902 | Inorg. Chem. 2011, 50, 12747−12761

same for both complex systems. The differences in the Pt−O bond length trans to X, where X is either NH or S (see drawing in Table 2), are mainly due to the stronger σ-labilization in case of **NSpy**, but have no influence on the first pK_{a1} value. Further differences can be seen in terms of the angles, where the major difference is related to angle β, the angle between the two platinum bound water ligands (see drawing in Table 2).

During deprotonation trans to the pyridine nitrogen donors, the angle between the two water molecules decreases more in the case of the **NNpy** system. Consequently, the necessary rearrangement in geometry after deprotonation is more favored in the **NSpy** system, where only small changes in geometry occur. Therefore, we assume that the resulting diaqua-dihydroxo **NSpy** species is more stable and consequently leads to lower pK_{a1} values compared to its N,N-analogues.

Kinetic Measurements with Thiourea. The kinetics of the substitution of coordinated water was investigated spectrophotometrically by following the change in absorbance at suitable wavelengths as a function of time. A pH of 2 was selected to guarantee the presence of tetra-aqua species in solution. The investigations act as preliminary tests to study the behavior of the aqua complexes and to compare the results for the series complexes with different chain length. By way of example, the absorbance changes observed during the reaction of 0.1 mM **10NSpy** with 5 mM thiourea are presented in Figure 8, and Figures S21−S23 (Supporting Information) show

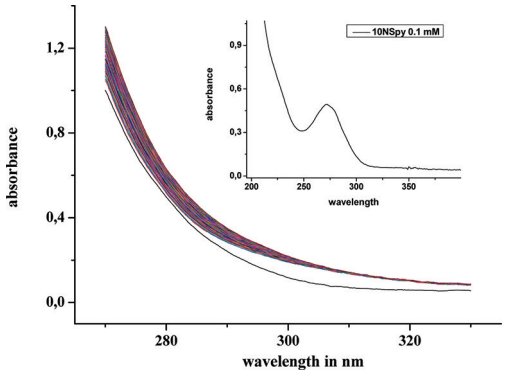

Figure 8. UV−vis spectra recorded during the reaction of 0.1 mM **10NSpy** with 5 mM thiourea at 25 °C and pH 2 (I = 0.01 M, triflic acid). Inset: absorbance spectrum of 0.1 mM **10NSpy** in the absence of thiourea.

the plots for the other three complexes. The spectra illustrate a large change in absorbance that results in an isosbestic point around 310 nm, which represents the first fast substitution step, followed by a steady increase in absorbance until the end of the reaction is reached. On the basis of the information obtained from these spectra, the wavelength 310 nm was selected to follow the first fast reaction and 290 nm was selected to observe the second slower substitution step. In addition, it should be pointed out that the N,S-system includes a stereogenic center at each sulfur donor atom SR_2. Yates et al. studied the behavior of the mononuclear NSpy complex [Pt(methylthiomethylpyridine)Cl_2] in solution using variable-temperature NMR spectroscopy.[60] Their experiments showed that the dichloro complex undergoes fluxional processes in solution at ambient temperature, which was confirmed by density functional theory (DFT) calculations to be mainly (S)-pyramidal inversion at the sulfur center. For the dinuclear system there is a long aliphatic chain instead of a methyl group. However, the chain is flexible and can easily undergo rotation and flipping. We, therefore, assume that the evidence of (S)-inversion is of significant importance in our case because it explains why in solution a mixture of all possible configurations was always observed and that it is impossible to isolate one of them in a pure form. Because the nucleophilic attack occurs above or below the square planar coordination sphere of the Pt(II) complexes, the configuration of the sulfur donor atom has no effect on the substitution rate.

In the kinetic measurements at least a 50-fold excess of thiourea relative to the complex concentration was used to guarantee pseudo-first-order conditions for the consecutive substitution reactions. Since it is known that triflate anions do not coordinate to Pt(II) metal centers,[61] 0.01 M triflic acid (pH 2) was used as solvent for all measurements, which leads to an ionic strength of I = 0.01 M. Furthermore, the pH of 2 was selected to guarantee the evidence of the tetra-aqua complex and to prevent the formation of hydroxo species, which are known to be inert against further substitution.[62,63] The time dependent spectra observed for the reactions of **4NSpy**, **6NSpy**, and **8NSpy** can be analyzed using a double-exponential fit, which indicates that there are two consecutive reactions observed at 310 nm (see Figures S24−S26, Supporting Information). The **10NSpy** complex is an exception in this respect and shows a different behavior compared to its shorter-bridged analogues in that it exhibits only one reaction step at 310 nm, which can be fitted by a single exponential function as illustrated in Figure S27, Supporting Information. This different behavior in kinetic reactivity fits perfectly to the information based on the pK_a values for **10NSpy** (see further discussion). At 290 nm, the data for the slowest reaction clearly shows a single exponential behavior for all four studied complexes because at this selected wavelength, the first rapid steps were not to be taken into account (see Figures S28−S31, Supporting Information). On using thiourea as a neutral nucleophile, the charge on the complex remains constant during the substitution steps, and because of the C_i-symmetry of the complexes, we expect two water ligands to be equivalent and substituted simultaneously.

In recent work, we performed a detailed study on the mononuclear NSpy complex (**Pt(mtp)**, see Figure 1).[32] This complex now acts as a reference for the here studied dinuclear system. In general, we found similar and well-established reactivity with thiourea as entering nucleophile. Especially the **10NSpy** complex with the longest methyl chain shows very similar behavior compared to **Pt(mtp)**, whereas the shorter-bridged complexes differ in reactivity. For the further discussion and for clarity concerning the introduced rate constants, we suggest the successive substitution steps outlined in Scheme 2 by way of a first approach.

Scheme 2. Suggested Substitution Mechanism for the Dinuclear Complex System with Thiourea (tu)

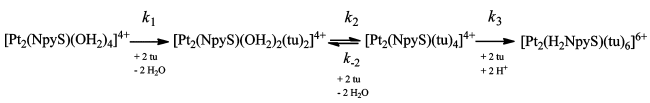

Because of the strong trans labilizing effect of the sulfur donor, the displacement of the water ligand trans to sulfur occurs in the first reaction step. For this step the different chain lengths have an influence on the rate of the substitution reaction. As the aliphatic chain becomes longer, more electron density is pushed into the metal center because of the inductive effect of the methylene groups, with the consequence that the

dx.doi.org/10.1021/ic2018902 | Inorg. Chem. 2011, 50, 12747−12761

Table 3. Summary of the Rate Constants and Activation Parameters for the Displacement of Coordinated Water by Thiourea at 25 °C and pH 2

	Pt(mtp)[32]	4NSpy	6NSpy	8NSpy	10NSpy
k_1 (M^{-1} s^{-1})	634 ± 10	252 ± 3	221 ± 5	211 ± 2	203 ± 5
k_2 (M^{-1} s^{-1})		18.8 ± 0.3	16.7 ± 0.1	17.7 ± 0.2	
k_{-2} (s^{-1})		0.031 ± 0.004	0.034 ± 0.001	0.033 ± 0.001	
k_3K_2 (M^{-2} s^{-1})	73.3 ± 0.8				23.1 ± 0.2
k_4K_3 (M^{-2} s^{-1})		24.9 ± 0.4	22.1 ± 0.6	21.8 ± 0.2	
$\Delta H^{\#}_1$ in kJ mol^{-1}	30 ± 1	34 ± 1	37.2 ± 0.3	39 ± 1	41.3 ± 0.4
$\Delta S^{\#}_1$ (J mol^{-1} K^{-1})	−90 ± 3	−84 ± 3	−71 ± 1	−66 ± 4	−61 ± 1
$\Delta H^{\#}_2$ (kJ mol^{-1})		48 ± 1	47 ± 2	47 ± 2	
$\Delta S^{\#}_2$ (J mol^{-1} K^{-1})		−59 ± 4	−63 ± 6	−64 ± 5	
$\Delta H^{\#}_{-2}$ (kJ mol^{-1})		65 ± 4	64 ± 2	64 ± 5	
$\Delta S^{\#}_{-2}$ (J mol^{-1} K^{-1})		−54 ± 13	−57 ± 7	−57 ± 16	
$\Delta H^{\#}_{2,3}$ (kJ mol^{-1})	12.5 ± 0.5				18.0 ± 0.3
$\Delta S^{\#}_{2,3}$ (J mol^{-1} K^{-1})	−169 ± 2				−158 ± 1
$\Delta H^{\#}_{3,4}$ (kJ mol^{-1})		18.8 ± 0.6	18.7 ± 0.8	18.2 ± 0.6	
$\Delta S^{\#}_{3,4}$ (J mol^{-1} K^{-1})		−155 ± 2	−155 ± 3	−157 ± 2	
$\Delta V^{\#}_1$ (cm^3 mol^{-1})	−5.5 ± 0.1	−7.5 ± 0.2	−6.96 ± 0.03	−5.6 ± 0.2	−4.73 ± 0.02
$\Delta V^{\#}_2$ (cm^3 mol^{-1})		−4.8 ± 0.2	−4.6 ± 0.2	−4.9 ± 0.3	
$\Delta V^{\#}_{-2}$ (cm^3)		−10.9 ± 0.5	−8.7 ± 0.2	−7.7 ± 0.2	

Pt(II) center becomes less electrophilic and the nucleophilic attack occurs slower. The described effect leads to a clear decrease in reactivity in the order **4NSpy** (252 M^{-1} s^{-1}) > **6NSpy** (221 M^{-1} s^{-1}) > **8NSpy** (211 M^{-1} s^{-1}) > **10NSpy** (203 M^{-1} s^{-1}) at 25 °C (also Table 3). The first substitution step for the Pt(mtp) complex is almost three times faster (634 M^{-1} s^{-1}), which is in good agreement with the obtained pK_a values and the reduced charge of 2+. The observed rate constants for the dinuclear systems and, for comparison, the rate constants for the mononuclear complex are summarized in Table 3, where eq 1 presents the rate law for the first substitution step.

$$k_{obs1} = k_1[tu] + k_{-1} \approx k_1[tu] \qquad tu = \text{thiourea} \tag{1}$$

The determined pseudo-first-order rate constants, k_{obs1}, were plotted against the thiourea concentration, and resulted in a linear dependence with no meaningful intercept as seen in Figure 9 (see also Table S8, Supporting Information). This indicates that the reverse reaction with water is too slow and can be neglected.

The subsequent reaction occurs trans to the pyridine unit and involves the displacement of the second water ligand at each Pt(II) center. This substitution step is about ten times slower compared to the first one, since the first thiourea ligand has already entered the coordination sphere, thereby increases the electron density on the Pt(II) center with its σ-donating ability, which results in a slower nucleophilic attack. Furthermore, the second step is not influenced by the bridging element. In consequence, we found nearly the same rate constants k_2 for the complexes **4NSpy** (18.8 M^{-1} s^{-1}), **6NSpy** (16.7 M^{-1} s^{-1}), and **8NSpy** (17.7 M^{-1} s^{-1} at 25 °C) within the standard error limits (see Table 3). Figure 10 shows plots of k_{obs2} against the nucleophile concentration, which result in a linear dependence with a small but clear intercept (see also Table S9, Supporting Information). The corresponding rate law is given in eq 2 and the values of k_2 and k_{-2} are summarized in Table 3.

$$k_{obs2} = k_2[tu] + k_{-2} \qquad tu = \text{thiourea} \tag{2}$$

The back reaction (k_{-2}) for the second substitution step can be accounted for in terms of the competing three sulfur σ-donor ligands at the Pt(II) center (viz. SR_2, first and second thiourea ligands), which leads to a labilization of the second entered thiourea ligand and displacement by water. Furthermore, the rate constants k_{-2} for the back reaction are the same within the experimental error limits (0.033 s^{-1}). No second substitution reaction on this time scale could be found for the **10NSpy** complex at 310 nm as mentioned above.

A final reaction step could be observed for all four dinuclear complexes at 290 nm. It is the second observed reaction step, k_{obs3}, for **10NSpy** and the third observed reaction step, k_{obs4}, for **4NSpy**, **6NSpy**, and **8NSpy**. All four complexes show nearly the same observed rate constants, $k_{obs3,4}$, for this final step (approximately 23 M^{-2} s^{-1} in terms of a third-order rate constant), from which we suggest that the final step involves dechelation of the pyridyl rings. The rate for dechelation does not depend on the length of the aliphatic chain because two thiourea ligands have already entered the Pt(II) coordination sphere and overrule the earlier effect of the aliphatic chain. Plots of the obtained rate constants, k_{obs3}, against the thiourea concentration lead to a square concentration dependence that is shown exemplarily in Figure 11 (see also Table S10, Supporting Information) for the **10NSpy** complex, and Figures S32−S34 (Supporting Information) show plots of k_{obs4} against the thiourea concentration for the **4NSpy**, **6NSpy**, and **8NSpy** complexes, which also result in square concentration dependences (see also Table S11, Supporting Information).

In summary, we observed a different reaction behavior for the **10NSpy** complex than for the shorter-bridged **NSpy** complexes, and they are therefore discussed separately. As known from the pK_a determination, the **4NSpy**, **6NSpy**, and **8NSpy** complexes involve platinum centers that can communicate among each other. Therefore, changes in charge during substitution reactions could play a crucial role. The first and the second reaction steps, k_1 and k_2, were found to be the displacement of coordinated water by neutral thiourea ligands and consequently the overall charge of 4+ remained constant. As seen in Scheme 3, the dechelation of one pyridine ring and the immediate protonation of the pyridine nitrogen atom lead

dx.doi.org/10.1021/ic2018902 | Inorg. Chem. 2011, 50, 12747−12761

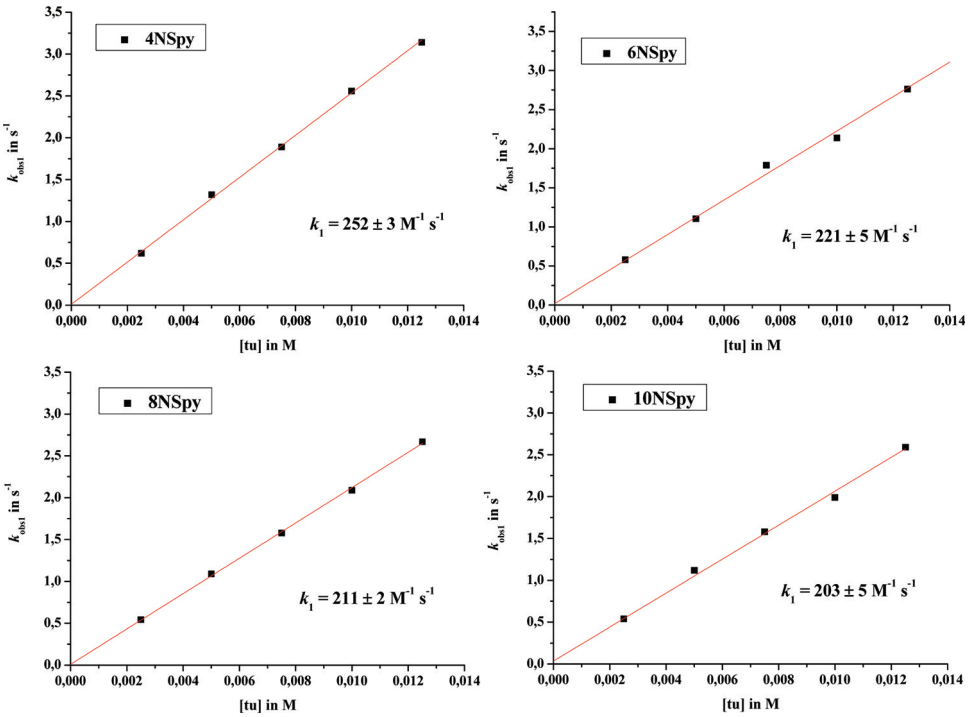

Figure 9. Plots of k_{obs1} vs thiourea concentration for the reaction with 0.1 mM complex in 0.01 M triflic acid (pH 2, I = 0.01 M) at 25 °C.

to an increase in charge from 4+ to 5+. Because of the interaction of the two Pt(II) centers, two dechelation steps are expected, where the first dechelation, k_3, occurs as a pre-equilibrium, K_3, followed by a fast second dechelation step, k_4. This behavior leads to a square concentration dependence, and the rate law for the third-order rate constant, k_4K_3, is given by eq 3.

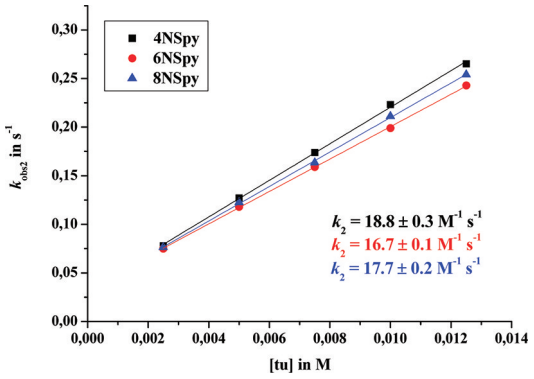

Figure 10. Plots of k_{obs2} vs thiourea concentration for the reaction with 0.1 mM of the **4NSpy**, **6NSpy**, and **8NSpy** complexes in 0.01 M triflic acid (pH 2, I = 0.01 M) at 25 °C.

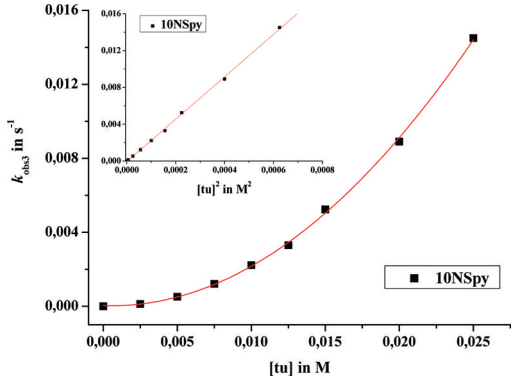

Figure 11. Plots of k_{obs3} vs thiourea concentration for the reaction with 0.1 mM **10NSpy** in 0.01 M triflic acid (pH 2, I = 0.01 M) at 25 °C. Inset: Plot of k_{obs3} vs $[\text{thiourea}]^2$ for the **10NSpy** complex.

$$k_{obs4} = \frac{k_4 \times K_3[tu]^2}{1 + K_3[tu]} \approx k_4K_3[tu]^2 \quad (\text{with } K_3 = k_3/k_{-3}) \tag{3}$$

The substitution of the second water molecule leads to three sulfur donor atoms at each Pt center. The remaining N_{py}–Pt bond is strongly labilized by the trans effect of the thiourea nucleophile. We, therefore, suggest that the third step—the dechelation of the NSpy ligand—happens fast. Moreover, fast dechelation is enforced by the immediate protonation of the free pyridine nitrogen atom. Fischer et al.[64] found a pK_a value of about 4.50 for such substituted pyridine derivatives. This means that at the studied pH of 2 the nitrogen atom of the pyridine ring is protonated and avoids rechelation, and therefore forces the reaction in one direction (Scheme 3).

It is known from the literature[65] that at a specific chain length the two metal centers within a dinuclear complex do not interact with each other anymore. The required chain length to reach two independent Pt(II) centers is different for each complex system. Therefore, we suggest that the **10NSpy** complex with the longest aliphatic chain behaves like a mononuclear complex and consequently has similar mechanistic properties to the **Pt(mtp)** reference complex as mentioned before. The observed behavior during the pH titration confirms this assumption. In a recent study,[32] we postulated for the **Pt(mtp)** complex that the displacement of the last water molecule and the dechelation of the pyridyl unit occur as a pre-equilibrium followed by a fast second step, which can not be separated from each other. This behavior results in a

dx.doi.org/10.1021/ic2018902 | Inorg. Chem. 2011, 50, 12747–12761

Scheme 3. Proposed Reaction Mechanism for the Reactions of 4NSpy, 6NSpy, and 8NSpy with Thiourea (n = 4, 6, and 8)

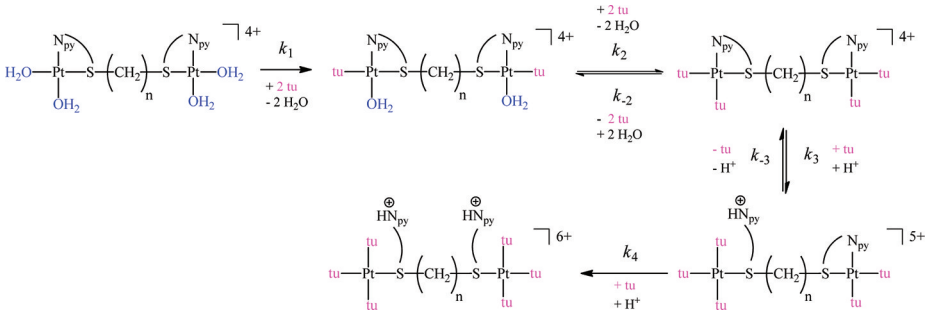

third-order rate constant with a square nucleophile concentration dependence.[32] Since the **10NSpy** complex behaves like the mononuclear reference complex, we suggest the same steady state process with a fast equilibrium ($K_2 = k_2/k_{-2}$), followed by an irreversible reaction with the rate constant k_3, which can be seen in Scheme 4. The last reaction is the

Scheme 4. Proposed Reaction Pathway Exclusively for the Reaction of 10NSpy Complex with Thiourea

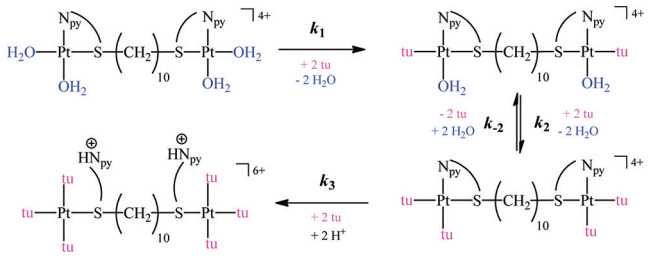

dechelation of the pyridyl rings. Because the Pt(II) centers do not interact with each other anymore, the change in charge has no influence on the substitution process, and dechelation occurs simultaneously for both pyridyl rings. The so-defined rate law is given in eq 4 and the obtained third-order rate constant, k_3K_2, for **10NSpy** is summarized in Table 3.

$$k_{obs3} = \frac{k_3 \times K_2[tu]^2}{1 + K_2[tu]} \approx k_3K_2[tu]^2 \quad (\text{with } K_2 = k_2/k_{-2}) \qquad (4)$$

Finally, we note that after coordination of a third thiourea ligand to each Pt(II) complex, the strong *trans*-labilizing effect of thiourea will also affect the thioether donor, which is the only connection in the dinuclear system. The excess of thiourea is large enough to displace the last donor in the ligand system to produce $[Pt(tu)_4]^{2+}$. However, this decomposition is very slow and was not studied in the present work.

Activation Parameters for the Reaction with Thiourea. In addition, temperature and pressure dependence studies were performed to gain more insight into the nature of the substitution mechanism from the thermal and pressure activation parameters. The thermal parameters $\Delta H^{\#}$ and $\Delta S^{\#}$ were determined by measuring the rate constants of the first and last substitution step of each complex at a fixed thiourea concentration as a function of temperature (Figures S35–S42 and Tables S12–S14, Supporting Information). Complete concentration dependence studies at different temperatures were performed for the second reaction step since it includes an intercept, namely, the back reaction (Figures S43–S51 and Tables S15–S21, Supporting Information). Figure 12 shows the Eyring plots for the three determined reaction steps

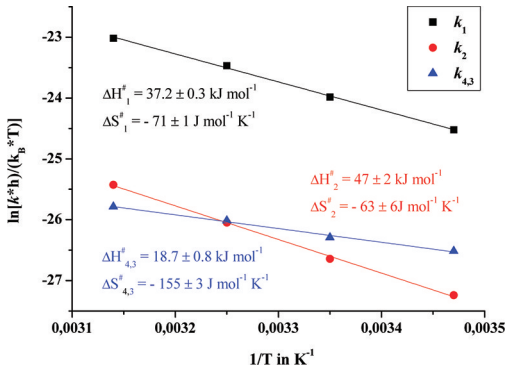

Figure 12. Eyring plots for the determination of the thermal activation parameters for the successive reaction steps of 0.1 mM **6NSpy** with thiourea at pH 2 (I = 0.01 M triflic acid).

exemplarily for the **6NSpy** complex. The data were calculated using the Eyring equation for which the observed first-order rate constants k_{obs1} were converted to second-order rate constants ($k = k_{obs}/[tu]$) based on eq 1 and converted to the third-order rate constants ($k = k_{obs}/[tu]^2$) based on eq 3, and the results are summarized in Table 3.

As expected, the activation enthalpy $\Delta H^{\#}_1$ and entropy $\Delta S^{\#}_1$ of the first reaction step increase with elongation of the aliphatic chain. This collaborates perfectly with the obtained rate constants. A slower reaction is accompanied by an unfavorably high transition state and therefore higher activation enthalpies and less negative activation entropies, thus a higher activation barrier. Only for the shorter-bridged complexes **4NSpy**, **6NSpy**, and **8NSpy** the displacement of the second water molecule at each Pt(II) center could be followed. In that case, the values of k_2 in general decrease compared to the rapid first step, which is also reflected in the activation parameters. The activation enthalpy as well as the activation entropy show lower values than for the first step. Moreover, nearly the same values for $\Delta H^{\#}_2$ (47 kJ mol^{-1}) and for $\Delta S^{\#}_2$ (−62 J mol^{-1} K^{-1}) can be found. Since the substitution reaction occurs trans to the pyridine nitrogen donor, the rate and activation parameters are not influenced by the chain length. The back reaction k_{-2} also shows similar activation parameters ($\Delta H^{\#}_{-2} \approx 64$ kJ mol^{-1} and $\Delta S^{\#}_{-2} \approx -57$ J mol^{-1} K^{-1}) for the three complexes, which means that the displacement of thiourea by water is also not influenced by the chain length. The same trend can be seen for the last step, $k_{3,4}$, for the shorter-bridged **NSpy** complexes. We found very similar values for $\Delta H^{\#}_{3,4}$ (18.5 kJ mol^{-1}) and for $\Delta S^{\#}_{3,4}$ (−155 J mol^{-1} K^{-1}), which again indicates that the third

dx.doi.org/10.1021/ic2018902 | Inorg. Chem. 2011, 50, 12747–12761

reaction step belongs to dechelation of the pyridine unit, which is independent of the bridging element. The stepwise dechelation of the first and second pyridine ring cannot be observed separately, and consequently the activation parameters $\Delta H^{\#}_{3,4}$ and $\Delta S^{\#}_{3,4}$ are composed of both steps. In addition, we note that the activation parameters for the displacement of the last water molecule and the simultaneous dechelation of both pyridine rings shows similar values for $\Delta H^{\#}_{2,3}$ and $\Delta S^{\#}_{2,3}$ in the case of **10NSpy**.

In addition, pressure dependence studies were performed for the first and second substitution steps by measuring the rate constants k_{obs1} for each complex at a fixed thiourea concentration (25 mM) as a function of pressure for the first step (Figures S52−S55 and Table S22, Supporting Information) and by performing a concentration dependence at different pressures for the second substitution step k_2 (Figures S56−S64 and Tables S23−S28, Supporting Information). The volumes of activation $\Delta V^{\#}$, calculated from the slope of plots of $\ln(k)$ versus pressure, are summarized in Table 3, and by way of example Figure 13 depicts plots of $\ln(k_{obs})$ versus pressure for the successive reaction steps of the **8NSpy** complex.

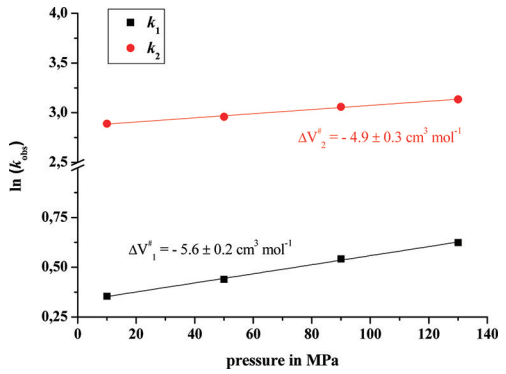

Figure 13. Plots of $\ln(k_{obs})$ vs pressure for the first and the second reaction steps of 0.1 mM **8NSpy** with 25 mM thiourea at 25 °C and pH 2 (I = 0.01 M triflic acid).

Throughout the series of complexes the substitution reactions were accelerated with increasing pressure. The so-obtained activation volumes are very typical for associative substitution reactions on square-planar complexes,[66−68] where the volume decrease results from bond formation on going from the square-planar reactant state to the trigonal bipyramidal transition state. This mechanistic assignment is furthermore in good agreement with the negative activation entropies found for the two reaction steps for all dinuclear complexes (see Table 3). The $\Delta V^{\#}_1$ values increase in the order **4NSpy** (−7.5 cm^3 mol^{-1}) < **6NSpy** (−6.96 cm^3 mol^{-1}) < **8NSpy** (−5.6 cm^3 mol^{-1}) < **10NSpy** (−4.73 cm^3 mol^{-1}) at 25 °C. Since the first substitution step takes place trans to the sulfur donor, the chain length has an influence on the activation volume $\Delta V^{\#}_1$. With elongation of the methylene bridge, more electron density is pushed into the metal center, which leads to a decrease in electrophilicity of the Pt(II) center. In consequence, the entering nucleophile is less attracted, which leads to a less associative transition state and therefore to smaller negative activation volumes. For the displacement of the second water ligand at each metal center the activation volume $\Delta V^{\#}_2$ could only be determined for the shorter-bridged complexes. This substitution step occurs trans to the pyridine unit and is therefore independent of the chain length. For this reason it is not surprising that we found very similar $\Delta V^{\#}_2$ values for **4NSpy**, **6NSpy**, and **8NSpy** as seen in Table 3. Since the second substitution reaction includes a back reaction, the activation volumes $\Delta V^{\#}_{-2}$ for the back reaction were determined and found to be significantly negative. We found a clear tendency for the activation volumes of the back reaction in the order **4NSpy** < **6NSpy** < **8NSpy**. However, in this case the change is not caused by electron donation, but in fact by charge effects. With elongation of the methylene chain, the overall charge at each Pt(II) center decreases. On using water as a weak nucleophile (compared to thiourea), we suggest that the slight change in charge has an influence on the activation volume $\Delta V^{\#}_{-2}$ such that the back reaction has a stronger associative character for the shorter aliphatic chain and therefore a slightly more electrophilic metal center.

Cytostatic Activity. Dr. Thomas Huhn from the University of Konstanz and his team performed cell tests for all four dinuclear Pt(II) tetra-chloro complexes. The cytotoxicity of the chloro complexes **5**−**8** (see Figure 2) was studied using the AlamarBlue assay in the human cervix carcinoma cell line HeLa S3. Of all new complexes tested only **8**, the complex with the longest methylene chain, showed cytostatic activity. We found an IC_{50} value of 21 ± 9 μM for complex **8**, which describes the concentration at which 50% of the cells remained viable with respect to the control (see Table S29, Supporting Information). The resulting dose−response curve for the HeLa S3 cell line is shown in Figure 14. Cisplatin was also tested as a reference

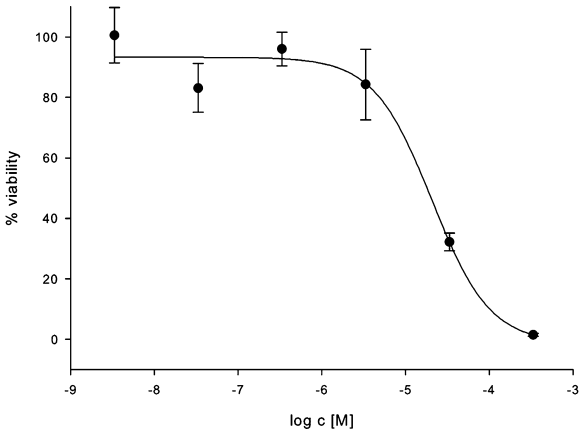

Figure 14. Dose−response curves for the HeLa S3 cell line for complex **8**.

compound and exhibited an IC_{50} value of 1.2 ± 0.4 μM. We note that the free ligand itself shows some cytotoxic activity (67 μM, not shown), but the IC_{50} values clearly show that complex **8** results in a much higher activity than the ligand.

The chloro complexes instead of the corresponding aqua species were used for the cell tests because of their biological and medical relevance. In general, a platinum drug such as cisplatin is injected into the body as the corresponding chloro species. On its way to the cell, the relatively high chloride concentration in blood and other tissues suppress the hydrolysis reactions. After entering the cell (influx), where a much lower chloride concentration is present, the platinum drug undergoes hydrolysis. It is nowadays well-accepted that the active species for cisplatin is [*cis*-Pt(NH$_3$)$_2$(OH$_2$)Cl]$^+$, where one labile water molecule can easily be displaced.[69] Determination of the pK_a values is therefore of special interest,

dx.doi.org/10.1021/ic2018902 | Inorg. Chem. 2011, 50, 12747−12761

Table 4. Summary of the Chemical Quantum Calculations for the Mononuclear and Dinuclear Complexes

	Pt(mtp)	4NSpy	6NSpy	8NSpy	10NSpy
Φ (S−C−H_2− C_{py}−N_{py}) (deg)	29.4	27.3	27.6	27.7	27.9
d Pt−S (Å)	2.30	2.31	2.31	2.31	2.31
d Pt−$O_{trans\ to\ S}$ (Å)	2.17	2.16	2.17	2.17	2.18
d Pt−N_{py} (Å)	2.00	2.01	2.01	2.01	2.01
d Pt−$O_{trans\ to\ py}$ (Å)	2.14	2.13	2.13	2.13	2.13
d Pt−Pt (Å)		10.81	13.33	15.88	18.40
d S−(CH_{2n}−S) (Å)		7.04	9.57	12.10	14.66

since if the water molecules at the metal center are too acidic, hydroxo species will be generated under physiologically relevant pH conditions and such complexes are known to be inert to further substitution reactions. On the basis of the pK_a values for the cytostatic active **10NSpy** complex, we know that at physiological pH the diaqua-dihydroxo species is present in solution, where one water and one hydroxo ligand are coordinated at each Pt(II) center.

The complexes with shorter aliphatic chains show no cytostatic activity. The mononuclear reference complex **Pt(mtp)** was found to be active.[31] We assume that the cytostatic activity derives from the same Pt(II) moiety, namely, the pyridine donor linked to a thioether donor. Furthermore, it was demonstrated from the pK_a determination that at a bridge length of 10 methylene groups the two Pt(II) metals do not interact with each other and behave like mononuclear compounds. However, the complex is dinuclear, and it is known from literature that polynuclear complexes exhibit different DNA adducts because of the ability to form long-ranged interstrand cross-links.[70] Widespread studies in cell-free systems indicate that the formation of interstrand cross-links is a major event for di- or polynuclear complexes.[19] Thus, dinuclear cytostatic active complexes may have the advantage of a different binding-mechanism to DNA. As mentioned above, they form long-ranged interstrand DNA-adducts and the so caused DNA-damage cannot be sufficiently repaired.[71] Consequently, polynuclear complexes may help in terms of overcoming Pt-drug resistance.

DFT Calculations. Table 4 summarizes the results of the quantum chemical calculations. The data show in general shorter Pt−N bonds than the Pt−O bonds, and of course the Pt−N_{py} bond is shorter than the Pt−S bond for each complex. Furthermore, the Pt−O bond trans to sulfur is longer than the Pt−O bond trans to N_{py} for each dinuclear complex. This nicely depicts the trans labilizing effect of the sulfur donor. The calculated dihedral angles (N_{py}−Pt···Pt−N_{py}) indicate a twist in the ring arrangement. An analysis of the calculated Pt−Pt distances show that two additional CH_2 groups add 2.52 Å to the Pt−Pt distance, which is very similar to the results of Ertürk et al.[57] and also perfectly comparable to the results of our recent work.[33] Because of the larger sulfur donor atoms, the Pt−Pt distances for all dinuclear N,S-complexes increases by 0.8 Å compared to the corresponding N,N-analogues (for more information concerning the **NNpy** system see ref 33).

By way of example, Figure 15 shows the calculated structure of the **4NSpy** complex (for the other structures see Figures S65−S68, Supporting Information). It is noticeable that the CH_2-group between the pyridine ring and the sulfur donor extremely sticks out of the square coordination sphere, and the bridging methylene chain behaves like a staggered zigzag chain.

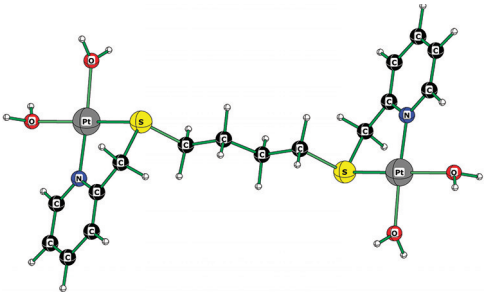

Figure 15. Calculated structure (B3LYP/LANL2DZp) (C_i) of the **4NSpy** complex.

CONCLUSIONS

In this study, a series of novel dinuclear platinum(II) complexes were synthesized containing a mixed nitrogen and sulfur donor bidentate chelate system. The two platinum centers are connected by an aliphatic chain of variable length by which the effect of elongating the methylene chain was studied. Furthermore, it was interesting to study the influence of combining a strong σ-donor and a π-acceptor within one complex system. We performed spectrophotometric acid−base titrations to determine the pK_a values for the coordinated water ligands. In general, we found four pK_a values for **4NSpy**, **6NSpy**, and **8NSpy**. The **10NSpy** complex with the longest methylene chain shows only two pK_a values. This can be ascribed to a clear correlation between chain length and acidity of platinum bound water. With elongation of the chain, the communication between the two Pt(II) centers becomes weaker and finally ends as seen for the **10NSpy** complex, which behaves like two mononuclear complexes with two equivalent water molecules at each metal center. Furthermore, we established a deprotonation pattern, where the first deprotonation occurs trans to the pyridine nitrogen donors and the last deprotonation occurs trans to the sulfur donors. Thereby, the first step is not influenced by the aliphatic chain length, whereas the last step shows increased pK_a values with increasing chain length, which can be accounted for by the increasing electron donation effect of the chain. On comparing the acidity of the N,S-complexes with their corresponding N,N-analogues, two differences are noted. The pK_a values of the **NSpy** system are approximately one pK unit lower, which can be explained by a more favored geometric arrangement following deprotonation. In contrast to **10NSpy**, the two Pt(II) centers can interact with each other in the case of the **10NNpy**. Kinetic measurements were performed with thiourea as a strong nucleophile under pseudo-first-order conditions as a function of nucleophile concentration, temperature, and pressure, using stopped-flow techniques and UV−vis spectroscopy. The different behavior of the shorter-bridged complexes and **10NSpy** during the pH titrations is also reflected in their

dx.doi.org/10.1021/ic2018902 | Inorg. Chem. 2011, 50, 12747−12761

kinetic reactivity. We found three successive reaction steps for the shorter-bridged **4NSpy**, **6NSpy**, and **8NSpy** complexes, which are ascribed to the stepwise displacement of water by thiourea, followed by a successive dechelation of the pyridine rings because of the favored protonation of the nitrogen atom under the selected experimental conditions. The reactivity of **10NSpy** is perfectly comparable to the mononuclear reference complex studied before.[32] Two reaction steps are observed that belong to the displacement of water by thiourea and finally to a simultaneous dechelation of both pyridine rings because of the lack of communication between the metal centers. Since the first substitution step occurs trans to the σ-donating sulfur, the results for k_1 indicate that there is a clear dependence on the aliphatic chain length. With elongation of the chain, more electron density is pushed onto the metal center, which leads to slower substitution reactions in the order **4NSpy** > **6NSpy** > **8NSpy** > **10NSpy**. Although the dechelation of one donor atom occurs relatively fast, we found the remaining $[Pt_2(H_2NpyS)(tu)_6]^{6+}$ species to be stable for at least 12 h. The final decomposition pattern of the complete system was not studied in this work.

It is known from the literature[34] that complexes with bidentate coordination spheres show higher cytostatic activity compared to their monodentate analogues with only one vacant coordination site. In addition, it is well-known from multinuclear complexes that the DNA adducts of such complexes are more flexible and long ranged, with a high degree of interstrand cross-links, and consequently are promising compounds to overcome cisplatin resistance.[35] Therefore, cytostatic cell tests for all dinuclear complexes were carried out using the HeLa S3 cell line, and the tetrachloro complex **8** with the longest chain was found to be cytostatic active with an IC_{50} value of 21 ± 9 μM.

■ ASSOCIATED CONTENT

Supporting Information

Figures S1−S7 show NMR spectra and Figures S87−S13 mass spectra of the dinuclear complexes. Figures S14−S16 summarize UV−vis spectra for the complexes **4NSpy**, **6NSpy**, and **10NSpy** in the pH range of 1−10, and Figures S17−S20 depict absorbance traces as a function of pH for all dinuclear complexes. Figures S21−S64 illustrate different UV−vis spectral changes, kinetic traces, concentration, temperature, and pressure dependent studies for all dinuclear complexes. Figures S65−S68 report the calculated structures of the dinuclear complexes. Tables S1−S4 summarize the fit reports for the pK_a determination, Tables S5−S8 depict the calculated bond lengths and angles, and Tables S8−S28 summarize all values of k_{obs} determined for all reactions as a function of nucleophile concentration, temperature, and pressure for all dinuclear complexes. Table S29 summarizes the experimental results for the cytostatic cell tests. This material is available free of charge via the Internet at http://pubs.acs.org.

■ AUTHOR INFORMATION

Corresponding Author

*E-mail: vaneldik@chemie.uni-erlangen.de.

■ ACKNOWLEDGMENTS

The authors gratefully acknowledge continued financial support from the Deutsche Forschungsgemeinschaft. The authors thank Dipl. Chem. Malin Bein and Dr. Thomas Huhn (Department of Chemistry and Konstanz Research School Chemical Biology, University of Konstanz, Germany) for help with the biological assays and the kind cooperation. Finally, the authors kindly thank Prof. Dr. Ivana Ivanović-Burmazović and Oliver Tröppner for their support with the mass spectrometric measurements and Dr. Achim Zahl for help with the ^{195}Pt-NMR measurements.

■ REFERENCES

(1) Wheate, N. J.; Walker, S.; Craig, G. E.; Oun, R. *Dalton Trans.* **2010**, *39*, 8113−8127.
(2) Rosenberg, B.; VanCamp, L.; Krigas, T. *Nature* **1965**, *205*, 698−699.
(3) Rosenberg, B.; VanCamp, L.; Trosko, J. E.; Mansour, V. H. *Nature* **1969**, *222*, 385−386.
(4) Neidle, S.; Ismail, I. M.; Sadler, P. J. *J. Inorg. Biochem.* **1980**, *13*, 205−212.
(5) Frey, U.; Ranford, J. D.; Sadler, P. J. *Inorg. Chem.* **1993**, *32*, 1333−1340.
(6) Wilkinson, R.; Cox, P. J.; Jones, M.; Harrap, K. R. *Biochimie* **1978**, *60*, 851−857.
(7) Cleare, M. J.; Hydes, P. C.; Malerbi, B. W.; Watkins, D. M. *Biochimie* **1978**, *60*, 835−850.
(8) Calvert, A. H.; Harland, S. J.; Newell, D. R.; Siddik, Z. H.; Jones, A. C.; McElwain, T. J.; Raju, S.; Wiltshaw, E.; Smith, I. E.; Baker, J. M.; Peckham, M. J.; Harrap, K. R. *Cancer Chemother. Pharmacol.* **1982**, *9*, 140−147.
(9) Evans, B. D.; Raju, K. S.; Calvert, A. H.; Harland, S. J.; Wiltshaw, E. *Cancer Treat. Rep.* **1983**, *67*, 997−1000.
(10) Barnard, C. F. J.; Cleare, M. J.; Hydes, P. C. *Chem. Brit.* **1986**, *22*, 1001−1004.
(11) Armand, J.-P.; Boige, V.; Raymond, E. *Semin. Oncol.* **2000**, *27*, 96−104.
(12) Extra, J. M.; Marty, M.; Brienza, S. *Semin. Oncol.* **1998**, *25*, 13−22.
(13) Kelland, L. *Nat. Rev. Cancer* **2007**, *7*, 573−584.
(14) Boulikas, T.; Vougiouka, M. *Oncol. Rep.* **2003**, *10*, 1663−1682.
(15) (a) Thompson, A. J.; Williams, R. J. P.; Reslova, S. *Struct. Bonding (Berlin)* **1972**, *11*, 1−46. (b) Sherman, S. E.; Lippard, S. J. *Chem. Rev.* **1987**, *87*, 1153−1181.
(16) Farrell, N.; de Almeida, S. G.; Skov, K. A. *J. Am. Chem. Soc.* **1988**, *110*, 5018−5019.
(17) Costa, L. A. S.; Rocha, W. R.; de Almeida, W. B.; Dos Santos, H. F. *J. Chem. Phys.* **2003**, *118*, 10584−10592.
(18) Farrell, N. *Comments Inorg. Chem.* **1995**, *16*, 373−389.
(19) Brabec, V.; Kašpárková, J.; Vrána, O.; Nováková, O.; Cox, J. W.; Qu, Y.; Farrell, N. *Biochemistry* **1999**, *38*, 6781−6790.
(20) Qu, Y.; Farrell, N. *J. Am. Chem. Soc.* **1991**, *113*, 4851−4857.
(21) (a) Farrell, N.; Qu, Y. *Inorg. Chem.* **1989**, *28*, 3416−3420. (b) Farrell, N.; Qu, Y.; Hacker, M. P. *J. Med. Chem.* **1990**, *33*, 2179−2184. (c) Roberts, J. D.; Van Houten, B.; Qu, Y.; Farrell, N. P. *Nucleic Acids Res.* **1989**, *17*, 9719−9733. (d) Kraker, A.; Elliott, W.; Van Houten, B.; Farrell, N.; Hoeschele, J.; Roberts, J. *J. Inorg. Biochem.* **1989**, *36*, 160.
(22) Roberts, J. D.; Beggiolin, G.; Manzotti, C.; Piazzoni, L.; Farrell, N. *J. Inorg. Biochem.* **1999**, *77*, 47−50.
(23) Roberts, J. D.; Peroutka, J.; Farrell, N. *J. Inorg. Biochem.* **1999**, *77*, 51−57.
(24) Bogdanović, G.; Kojić, V.; Srdić, T.; Jakimov, D.; Djuran, M.; Burgarčić, Ž. D.; Baltić, M.; Baldić, V. V. *Metal-Based Drugs* **2002**, *9*, 33−43.
(25) Mandal, S.; Castiñeiras, A.; Mondal, T. K.; Mondal, A.; Chattopadhyay, D.; Goswami, S. *Dalton Trans.* **2010**, *39*, 9514−9522.
(26) Pitteri, B.; Bortoluzzi, M.; Marangoni, G. *Trans. Met. Chem.* **2005**, *30*, 1008−1013.
(27) (a) Burgarčić, Ž. D.; Soldatović, T.; Jelić, R.; Alguerό, B.; Grandas, A. *Dalton Trans.* **2004**, *22*, 3869−3877. (b) Annibale, G.; Brandolisio, M.; Pitteri, B. *Polyhedron* **1995**, *14*, 451−453.

(28) Baldo, A.; Chessa, G.; Marangoni, G.; Pitteri, B. *Polyhedron* **1985**, *4*, 1429−1431.
(29) Jones, R. C.; Madden, R. L.; Skelton, B. W.; Tolhurst, V.-A.; White, A. H.; Williams, A. M.; Wilson, A. J.; Yates, B. F. *Eur. J. Inorg. Chem.* **2005**, *6*, 1048−1055.
(30) Jones, R. C.; Skelton, B. W.; Tolhurst, V.-A.; White, A. H.; Wilson, A. J.; Canty, A. J. *Polyhedron* **2007**, *26*, 708−718.
(31) Du Preez, J. G. H. *Platinum(II) complexes, preparation and use.* Document number: CA Patent 2547275, 2005; p 38.
(32) Hochreuther, S.; Nandibewoor, S. T.; Puchta, R.; van Eldik, R. *Dalton Trans.* **2011**, in press.
(33) Hochreuther, S.; Puchta, R.; van Eldik, R. *Inorg. Chem.* **2011**, *50*, 8984−8996.
(34) Qu, Y.; Farrell, N. *J. Am. Chem. Soc.* **1991**, *113*, 4851−4857.
(35) (a) Kloster, M. B. G.; Hannis, J. C.; Mudiman, D. C.; Farrell, N. *Biochemistry* **1999**, *38*, 14731−14737. (b) Brabec, V.; Kašpárková, J.; Vrána, O.; Nováková, O.; Cox, J. W.; Farrell, N. *Biochemistry* **1999**, *38*, 6781−6790. (c) Kašpárková, J.; Zehnulova, J.; Farrell, N.; Brabec, V. *J. Biol. Chem.* **2002**, *277*, 48076−48086. (d) Qu, Y.; Scarsdale, N. J.; Tran, M.-C.; Farrell, N. P. *J. Biol. Inorg. Chem.* **2003**, *8*, 19−28. (e) Qu, Y.; Scarsdale, N. J.; Tran, M.-C.; Farrell, N. *J. Inorg. Biochem.* **2004**, *98*, 1585−1590. (f) Hegmans, A.; Berners-Price, S. J.; Davies, M. S.; Thomas, D. S.; Humphreys, A. S.; Farrell, N. *J. Am. Chem. Soc.* **2004**, *126*, 2166−2180. (g) Qu, Y.; Tran, M.-C.; Farrell, N. P. *J. Biol. Inorg. Chem.* **2009**, *14*, 969−977.
(36) Hofmann, A.; Dahlenburg, L.; van Eldik, R. *Inorg. Chem.* **2003**, *42*, 6528−6538.
(37) (a) Reedijk, J. *Chem. Commun.* **1996**, 801−806. (b) Burchenal, J. H.; Kalaher, K.; Dew, K.; Lokys, L.; Gale, G. *Biochimie* **1978**, *60*, 961−965.
(38) Sarkar, S.; Patra, A.; Drew, M. G. B.; Zangrando, E.; Chattopadhyay, P. *Polyhedron* **2009**, *28*, 1−6.
(39) (a) Horie, M.; Sakano, T.; Osakada, K. *J. Organomet. Chem.* **2006**, *691*, 5935−5945. (b) Bierer, D. E.; Dener, J. F.; Dubenko, L. G.; Gerber, R. E.; Litvak, J.; Peterli, S.; Peterli-Roth, P.; Truong, T. V.; Mao, G.; Bauer, B. E. *J. Med. Chem.* **1995**, *38*, 2628−2648. (c) Gerber, R. E.; Hasbun, C.; Dubenko, L. G.; King, M. F.; Bierer, D. E. *Org. Synth. Coll. X* **2004**, *234*−*239*, 186−196.
(40) Djuran, M. I.; Milinkovic, S. U.; Habtemariam, A.; Parsons, S.; Sadler, P. J. *J. Inorg. Biochem.* **2002**, *88*, 268−273.
(41) Hofmann, A.; van Eldik, R. *Dalton Trans.* **2003**, *15*, 2979−2985.
(42) Hamid, R.; Rotshteyn, Y.; Rabadi, L.; Parikh, R.; Bullock, P. *Toxicol. In Vitro* **2004**, *18*, 703−710.
(43) van Eldik, R.; Gaede, W.; Wieland, S.; Kraft, J.; Spitzer, M.; Palmer, D. A. *Rev. Sci. Instrum.* **1993**, *64*, 1355−1357.
(44) Becke, A. D. *J. Chem. Phys.* **1993**, *98*, 564−5652.
(45) Stephens, P. J.; Devlin, F. J.; Chabalowski, C. F.; Frisch, M. J. *J. Phys. Chem.* **1994**, *98*, 11623−11627.
(46) Lee, C.; Yang, W.; Parr, R. G. *Phys. Rev. B: Condens. Matter Mater. Phys.* **1988**, *37*, 785−789.
(47) Dunning, T. H.; Hay, P. J. In *Modern Theoretical Chemistry*; Plenum: New York, 1976; Vol. 3, pp 1−28.
(48) (a) Hay, P. J.; Wadt, W. R. *J. Chem. Phys.* **1985**, *82*, 270−283. (b) Wadt, W. R.; Hay, P. J. *J. Chem. Phys.* **1985**, *82*, 284−298.
(49) Hay, P. J.; Wadt, W. R. *J. Chem. Phys.* **1985**, *82*, 299−310.
(50) Huzinaga, S., Ed.; *Gaussian Basis Sets for Molecular Calculations*; Elsevier: Amsterdam, The Netherlands, 1984.
(51) Frisch, M. J.; Trucks, G. W.; Schlegel, H. B.; Scuseria, G. E.; Robb, M. A.; Cheeseman, J. R.; Montgomery Jr., J. A.; Vreven, T.; Kudin, K. N.; Burant, J. C.; Millam, J. M.; Iyengar, S. S.; Tomasi, J.; Barone, V.; Mennucci, B.; Cossi, M.; Scalmani, G.; Rega, N.; Petersson, G. A.; Nakatsuji, H.; Hada, M.; Ehara, M.; Toyota, K.; Fukuda, R.; Hasegawa, J.; Ishida, M.; Nakajima, T.; Honda, J.; Kitao, O.; Nakai, H.; Klene, M.; Li, X.; Knox, J. E.; Hratchian, H. P.; Cross, J. B.; Bakken, V.; Adamo, C.; Jaramillo, J.; Gomperts, R.; Stratmann, E.; Yazyev, O.; Austin, A. J.; Cammi, R.; Pomelli, C.; Ochterski, J. W.; Ayala, P. Y.; Morokuma, K.; Voth, G. A.; Salvador, P.; Dannenberg, J. J.; Zakrzewski, V. G.; Dapprich, S.; Daniels, A. D.; Strain, M. C.; Farkas, O.; Malick, D. K.; Rabuck, A. D.; Raghavachari, K.; Foresman, J. B.; Ortiz, J. V.; Cui, Q.; Baboul, A., G.; Clifford, S.; Cioslowski, J.; Stefanov, B. B.; Liu, G.; Liashenko, A.; Piskorz, P.; Komaromi, I.; Martin, R. L.; Fox, D. J.; Keith, T.; Al-Laham, M. A.; Peng, C. Y.; Nanayakkara, A.; Challacombe, M.; Gill, P. M. W.; Johnson, B.; Chen, W.; Wong, M. W.; Gonzalez, C.; Pople, J. A. *Gaussian 03*, Revision B.03; Gaussian Inc.: Wallingford, CT, 2004.
(52) (a) Qu, Y.; Farrell, N. *J. Inorg. Biochem.* **1990**, *40*, 255−264. (b) Khokhar, A. R.; Deng, Y.; Al-Baker, S.; Yoshida, M.; Siddik, Z. H. *J. Inorg. Biochem.* **1993**, *51*, 677−687. (c) Shen, W.-Z.; Schneckbeck, R.-D.; Freisinger, E.; Lippert, B. *Dalton Trans.* **2008**, *30*, 4044−4049. (d) Pizarro, A. M.; Munk, V. P.; Navarro-Ranninger, C.; Sadler, P. J. *Angew. Chem., Int. Ed.* **2003**, *42*, 5339−5342.
(53) Lee, K. W.; Martin, D. S. *Inorg. Chim. Acta* **1976**, *17*, 105−110.
(54) Lim, M. C.; Martin, R. B. *J. Inorg. Nucl. Chem.* **1976**, *38*, 1911−1914.
(55) Faggiani, R.; Lippert, B.; Lock, C. J. L.; Rosenberg, B. *J. Am. Chem. Soc.* **1977**, *99*, 777−781.
(56) Davies, M. S.; Cox, J. W.; Berners-Price, S. J.; Barklage, W.; Qu, Y.; Farrell, N. *Inorg. Chem.* **2009**, *39*, 1710−1715.
(57) Ertürk, H.; Hofmann, A.; Puchta, R.; van Eldik, R. *Dalton Trans.* **2007**, *22*, 2295−2301.
(58) Hofmann, A.; Jaganyi, D.; Munro, O. Q.; Liehr, G.; van Eldik, R. *Inorg. Chem.* **2003**, *42*, 1688−1700.
(59) Soldatović, T.; Bugarčić, Ž. D.; van Eldik, R. *Dalton Trans.* **2009**, *23*, 4526−4531.
(60) Jones, R. C.; Madden, R. L.; Skelton, B. W.; Tolhurst, V.-A.; White, A. H.; Williams, A. M.; Wilson, A. J.; Yates, B. F. *Eur. J. Inorg. Chem.* **2005**, *6*, 1048−1055.
(61) Fallis, S.; Anderson, G. K.; Rath, N. P. *Organometallics* **1991**, *10*, 3180−3184.
(62) Mahal, G.; van Eldik, R. *Inorg. Chem.* **1985**, *24*, 4165−4170.
(63) Mahal, G.; van Eldik, R. *Inorg. Chem.* **1987**, *127*, 203−208.
(64) Fischer, A.; King, M. J.; Robinson, F. P. *Can. J. Chem.* **1978**, *56*, 3059−3067.
(65) Davies, M. S.; Cox, J. W.; Berners-Price, S. J.; Barklage, W.; Qu, Y.; Farrell, N. *Inorg. Chem.* **2000**, *39*, 1710−1715.
(66) Stochel, G.; van Eldik, R. *Coord. Chem. Rev.* **1999**, *187*, 329−374.
(67) Helm, L.; Elding, L. I.; Merbach, A. E. *Helv. Chim. Acta* **1984**, *67*, 1453−1460.
(68) Helm, L.; Elding, L. I.; Merbach, A. E. *Helv. Chim. Acta* **1985**, *24*, 1719−1721.
(69) Berners-Price, S. J.; Appleton, T. G. *Platinum-based Drugs in Cancer Therapy*; Kelland, L. R., Farrell, N. P., Eds.; Humana Press Inc.: Totowa, N.J., 2000.
(70) (a) Cox, J. W.; Berners-Price, S. J.; Davies, M. S.; Qu, Y.; Farrell, N. *J. Am. Chem. Soc.* **2001**, *123*, 1316−1326. (b) Brabec, V.; Kasparova, J. *Drug Resist. Updates* **2005**, *8*, 131−146.
(71) (a) Kloster, M. B. G.; Hannis, J. C.; Mudiman, D. C.; Farrell, N. *Biochemistry* **1999**, *38*, 14731−14737. (b) Kašpárková, J.; Zehnulova, J.; Farrell, N.; Brabec, V. *J. Biol. Chem.* **2002**, *277*, 48076−48086. (c) Qu, Y.; Scarsdale, N. J.; Tran, M.-C.; Farrell, N. P. *J. Biol. Inorg. Chem.* **2003**, *8*, 19−28. (d) Qu, Y.; Scarsdale, N. J.; Tran, M.-C.; Farrell, N. *J. Inorg. Biochem.* **2004**, *98*, 1585−1590. (e) Hegmans, A.; Berners-Price, S. J.; Davies, M. S.; Thomas, D. S.; Humphreys, A. S.; Farrell, N. *J. Am. Chem. Soc.* **2004**, *126*, 2166−2180. (f) Qu, Y.; Tran, M.-C.; Farrell, N. P. *J. Biol. Inorg. Chem.* **2009**, *14*, 969−977.